Calcium release through P2X4 activates calmodulin to promote endolysosomal membrane fusion

Qi Cao,[1] Xi Zoë Zhong,[1] Yuanjie Zou,[1] Ruth Murrell-Lagnado,[2] Michael X. Zhu,[3] and Xian-Ping Dong[1]

[1]Department of Physiology and Biophysics, Dalhousie University, Halifax B3H 4R2, Nova Scotia, Canada
[2]Department of Pharmacology, University of Cambridge, Cambridge CB2 1PD, England, UK
[3]Department of Integrative Biology and Pharmacology, The University of Texas Health Science Center at Houston, Houston, TX 77030

Intra-endolysosomal Ca^{2+} release is required for endolysosomal membrane fusion with intracellular organelles. However, the molecular mechanisms for intra-endolysosomal Ca^{2+} release and the downstream Ca^{2+} targets involved in the fusion remain elusive. Previously, we demonstrated that endolysosomal P2X4 forms channels activated by luminal adenosine triphosphate in a pH-dependent manner. In this paper, we show that overexpression of P2X4, as well as increasing endolysosomal P2X4 activity by alkalinization of endolysosome lumen, promoted vacuole enlargement in cells and endolysosome fusion in a cell-free assay. These effects were prevented by inhibiting P2X4, expressing a dominant-negative P2X4 mutant, and disrupting the P2X4 gene. We further show that P2X4 and calmodulin (CaM) form a complex at endolysosomal membrane where P2X4 activation recruits CaM to promote fusion and vacuolation in a Ca^{2+}-dependent fashion. Moreover, P2X4 activation-triggered fusion and vacuolation were suppressed by inhibiting CaM. Our data thus suggest a new molecular mechanism for endolysosomal membrane fusion involving P2X4-mediated endolysosomal Ca^{2+} release and subsequent CaM activation.

Introduction

Lysosomes are intracellular organelles involved in breaking down endocytosed or phagocytosed materials, excess macromolecules, cellular debris, and damaged organelles using acid hydrolases. To accomplish these functions, lysosomes frequently fuse with other organelles, such as endosomes, autophagosomes, and phagosomes (Luzio et al., 2007b; Saftig and Klumperman, 2009). Evidence also suggests a homotypic fusion between lysosomes (Bakker et al., 1997). As with the synaptic vesicle fusion with the plasma membrane (PM), lysosome fusion is Ca^{2+} dependent (Peters and Mayer, 1998; Pryor et al., 2000; Piper and Luzio, 2004; Hay, 2007; Luzio et al., 2007a; Cheng et al., 2010; Lloyd-Evans and Platt, 2011; Morgan et al., 2011; Pittman, 2011). It has been suggested that the lysosome itself provides the main Ca^{2+} source, which upon release initiates both homotypic and heterotypic lysosome fusion (Pryor et al., 2000; Morgan et al., 2011). However, the molecular identities of lysosomal Ca^{2+} release channels and the Ca^{2+} sensor proteins involved in the fusion remain elusive.

Recently, several Ca^{2+}-permeable channels have been shown to localize to membranes of late endosome and lysosome (LEL). These include TRPML1 (transient receptor potential mucolipin 1; Dong et al., 2008, 2010; Cheng et al., 2010; Shen

et al., 2011), TRPM2 (transient receptor potential melastatin 2; Lange et al., 2009; Sumoza-Toledo et al., 2011), TPC2 (two-pore channel 2; Calcraft et al., 2009; Grimm et al., 2014), and P2X4 purinoceptor (Qureshi et al., 2007; Huang et al., 2014). Both TRPML1 and TRPM2 belong to the superfamily of transient receptor potential cation channels. Mutations in the TRPML1 gene lead to enlarged LELs (Chen et al., 1998; Cheng et al., 2010). We showed recently that TRPML1 is activated by phosphatidylinositol 3,5-bisphosphate (PI(3,5)P2), an LEL-specific PIP2. Interestingly, cells deficient of PI(3,5)P2 also exhibited enlarged LELs (Cheng et al., 2010; Dong et al., 2010), and this was rescued by TRPML1 overexpression (Dong et al., 2010). Therefore, the function of TRPML1 is tightly linked to PI(3,5)P2. Given that in yeast vacuoles, the counterpart of mammalian lysosomes, PI(3,5)P2 up-regulation is associated with fission (Rudge et al., 2004; Efe et al., 2005), TRPML1 may also play a function in LEL fission rather than fusion in higher eukaryotic cells, which would be consistent with the early notion on the importance of TRPML1 in lysosome biogenesis (Treusch et al., 2004). Supporting this argument, TRPML1-overexpressing cells do not display enlarged LELs even in the presence of the TRPML1 agonist, ML-SA1 (unpublished data).

TRPM2 was found to function as a LEL Ca^{2+}-release channel in pancreatic β cells (Lange et al., 2009) and dendritic

Correspondence to Xian-Ping Dong: xpdong@dal.ca

Abbreviations used in this paper: ALG-2, apoptosis-linked gene-2; Baf-A1, bafilomycin-A1; co-IP, coimmunoprecipitation; CRISPR, clustered regularly interspaced short palindromic repeat; GPN, glycyl-phenylalanine 2-naphthylamide; LEL, late endosome and lysosome; MA, methylamine; PI(3,5)P2, phosphatidylinositol 3,5-bisphosphate; PM, plasma membrane; PNF, postnuclear fraction; Syt VII, synaptotagmin VII; TEM, transmission EM; WT, wild type.

cells (Sumoza-Toledo et al., 2011). However, our repeated attempts using whole-lysosome patch clamp recording have failed to detect any TRPM2-like current in LEL isolated from either wild-type (WT) Cos1 cells or Cos1 cells that heterologously expressed TRPM2 (unpublished data). Therefore, TRPM2 might only function as a LEL Ca^{2+} release channel in specific cell types.

TPC2 was shown to mediate LEL Ca^{2+} release in response to nicotinic acid adenine dinucleotide phosphate (Calcraft et al., 2009). More recent studies using whole-lysosome recordings also suggested that TPC2 conducts mainly Na^+ with limited Ca^{2+} permeability in response to PI(3,5)P2 (Wang et al., 2012; Cang et al., 2013). Although a role for TPC2 in endolysosomal trafficking and fusion has been implicated (Ruas et al., 2010; Grimm et al., 2014; Lin-Moshier et al., 2014), exactly how it facilitates vesicle fusion remains unclear.

P2X receptors are commonly known as PM channels activated by ATP from the extracellular site (Qureshi et al., 2007; Khakh and North, 2012). Of the seven P2X receptors known to date, P2X4 has been found to be also localized intracellularly to LEL membranes where it is activated by luminal ATP in a pH-dependent manner (Qureshi et al., 2007; Huang et al., 2014). However, the unique roles of LEL P2X4 to LEL physiology remain to be explored.

In addition to the lack of knowledge on the Ca^{2+} release channel, the molecular identity of the Ca^{2+} sensor involved in LEL fusion also remains elusive. Three Ca^{2+}-binding proteins, CaM (Colombo et al., 1997; Peters and Mayer, 1998), synaptotagmin VII (Syt VII; Martinez et al., 2000), and apoptosis-linked gene-2 (ALG-2) have been proposed to function as Ca^{2+} sensors that regulate intracellular membrane trafficking. CaM may serve as the Ca^{2+} sensor that mediates homotypic fusion of early endosomes in mammalian cells (Colombo et al., 1997) and vacuole fusion in yeast (Peters and Mayer, 1998). Syt VII has been implicated in the fusion between lysosomes and the PM (Martinez et al., 2000). ALG-2 is a Ca^{2+}-binding protein of the penta-EF-hand protein family that has been suggested to interact with TRPML1 and play a role in the regulation of trafficking along the endosomal pathway (Vergarajauregui et al., 2009). Because CaM (Nielsen et al., 1987), Syt VII (Martinez et al., 2000), and ALG-2 (Vergarajauregui et al., 2009) are all localized to LEL, they might serve as Ca^{2+} sensors for LEL fusion (and/or fission).

Here, we show that both P2X4 and CaM contribute significantly to LEL fusion. P2X4 and CaM form a signaling complex in LEL, where Ca^{2+} released through P2X4 activates CaM to promote vesicle fusion. Our study demonstrates, for the first time, that LEL Ca^{2+} release via P2X4 channels plays an important role in LEL membrane fusion through a CaM-dependent mechanism.

Results

The role of P2X4 in membrane trafficking

We recently showed that the LEL-localized P2X4 receptors are activated by luminal ATP in a pH-dependent manner (Qureshi et al., 2007; Huang et al., 2014). As a Ca^{2+}-permeable channel, LEL P2X4 may contribute to LEL trafficking. To test this possibility, Cos1 cells were transfected with GFP-tagged rat P2X4 (rP2X4-GFP) and then loaded with Texas red 10-kD dextran for 3 h, followed by a 2 h chase, to label LEL (Weinert et al., 2010). We found that expressing rP2X4-GFP, but not Lamp1-GFP

(Fig. 1 A) or the nonfunctional mutant rP2X4-S341W-GFP (a dead mutant without a dominant-negative effect; Fig. S1 A; Silberberg et al., 2005; Qureshi et al., 2007; Huang et al., 2014), resulted in the formation of many large size vacuoles. Because of the spatial resolution limit of light microscopy, only vacuoles with diameters >2 µm were clearly resolvable and counted, which showed that P2X4 overexpression caused a similar trend of increase in vacuoles of different sizes (Fig. 1 C). Quantification of vacuolated cells, defined as those containing greater than three vacuoles with diameters >2 µm, revealed that they amounted for 31.2 ± 0.9% cells expressing rP2X4-GFP but only 8.4 ± 1.0% cells expressing Lamp1-GFP (Fig. 1 D) and 12.0 ± 1.9% cells expressing rP2X4-S341W-GFP (Fig. S1 A). Calculating the mean LEL diameters at per cell base also revealed the same promoting effect of P2X4 overexpression on vacuolation (Fig. S1 B). Because quantification of vacuolated cells revealed essentially the same effect on vacuolation as the more elaborated methods that require diameter measurement of individual vacuoles, it is used for all subsequent analysis.

We showed previously that LEL P2X4 activity was inhibited at the pH commonly found in LEL lumen despite the presence of sufficient ATP in these acidic organelles (Stoop et al., 1997; Huang et al., 2014). We reasoned that if P2X4 activation facilitated vacuolation, alkalization of LEL lumen should remove the low pH inhibition, resulting in enhanced LEL P2X4 activity and increased vacuolation. Therefore, the dextran-loaded cells were treated with 10 mM methylamine (MA), 10 mM NH_4Cl, or 200 nM bafilomycin-A1 (Baf-A1) to increase luminal pH (Poole and Ohkuma, 1981; Tapper and Sundler, 1995; Christensen et al., 2002; Qureshi et al., 2007). As expected, all three treatments led to vacuolation in a time-dependent manner, approaching saturation in ∼60 min (Fig. S1, C–E). After the 60-min MA treatment, vacuolated cells accounted for 75.5 ± 3.5% of rP2X4-GFP–expressing cells, which is significantly higher than those that expressed Lamp1-GFP (53.79 ± 5.48%; Fig. 1, B–D). Similarly, the 60-min treatment with Baf-A1 led to vacuolation in 71.3 ± 4.6% rP2X4-GFP–expressing cells, again significantly higher than in Lamp1-GFP–expressing cells (Fig. 1, C and D). Importantly, after the drug treatment the percentage of vacuolated cells was similar between untransfected WT cells and cells expressing Lamp1-GFP (Fig. 1 D), indicating that the increased vacuolation detected in the rP2X4-GFP cells was caused by expression of rP2X4 rather than just any GFP-tagged LEL membrane protein. Collectively, these data suggest that activation of LEL P2X4 facilitates vacuolation.

To further confirm that P2X4 channel activity is required for increased vacuolation, rP2X4-GFP was coexpressed with its dominant-negative mutant P2X4-C353W-GFP (Fig. S2 A; Silberberg et al., 2005; Guo et al., 2007; Huang et al., 2014), and this dramatically reduced vacuolation (Fig. 1 D). The effect was not mimicked by coexpression with Lamp1-GFP or P2X4-S341W-GFP (Fig. S1 F), ruling out the possibility that the rescue against MA- and Baf-A1–induced vacuolation was because of a competition on the expression of heterologous proteins. It has been shown that the H286A mutation alters the pH regulation of P2X4 channel (Clarke et al., 2000). Indeed, in whole-lysosome recordings, the P2X4-H286A mutant exhibited significant current with a pH 4.6 pipette solution, whereas the WT channel was totally inhibited under the same conditions (Fig. S2 B). Consistent with the higher basal activity in LEL, expressing rP2X4-H286A-GFP in Cos1 cells led to stronger vacuolation than expressing rP2X4-GFP under normal culture
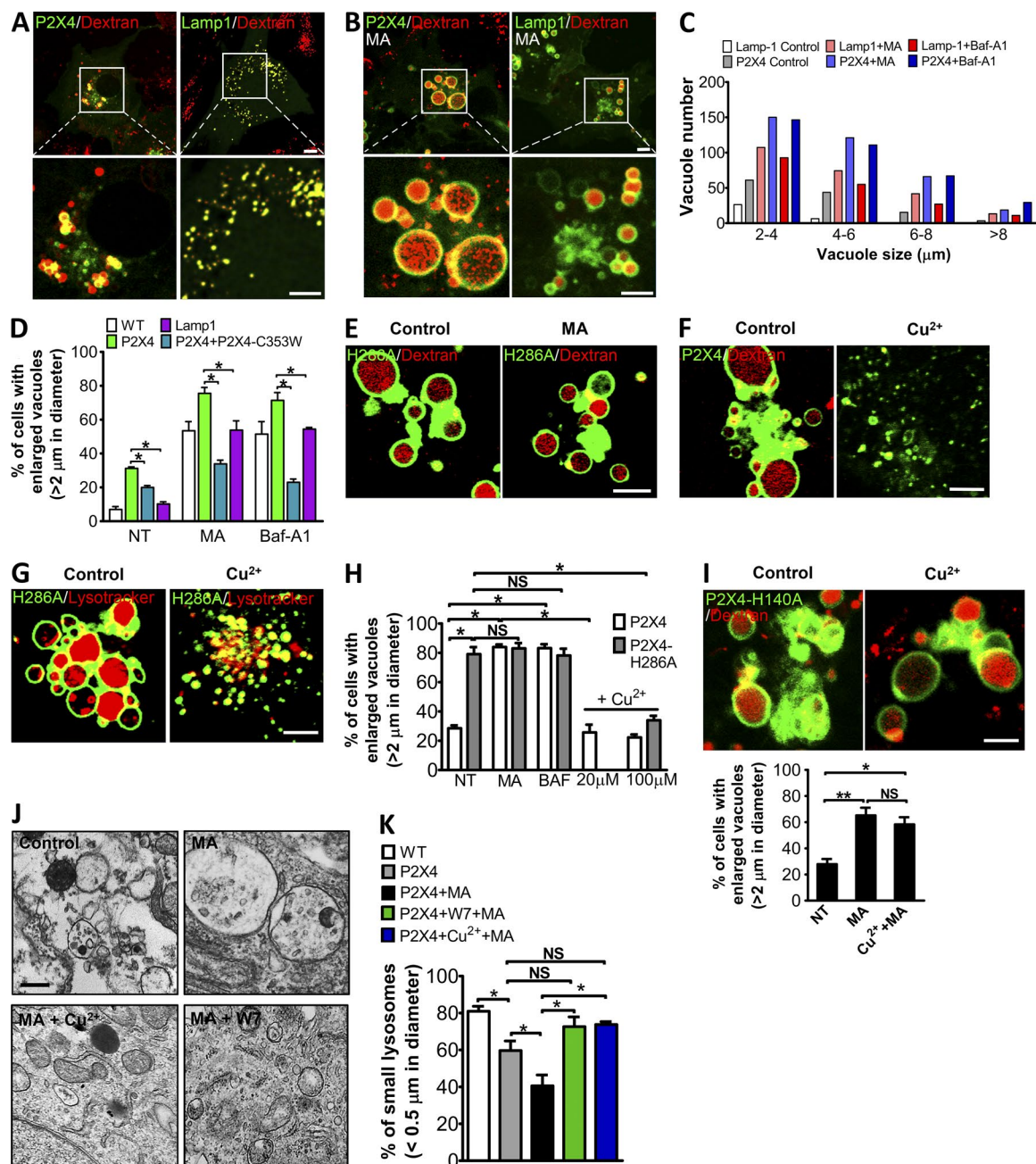
Figure 1. **Alkalinization induced LEL vacuolation in a P2X4-dependent manner.** (A–D) Cos1 cells were transiently transfected with Lamp1-GFP, rP2X4-GFP, or its dominant-negative mutant rP2X4-C353W-GFP. LELs were labeled with Texas red 10-kD dextran. (A) Expression of rP2X4-GFP increased LEL vacuole sizes as compared with Lamp1-GFP. (B) 10 mM MA (1 h) treatment caused vacuole enlargement in cells that expressed rP2X4-GFP or Lamp1-GFP. (C) Histogram for vacuole size distributions under the conditions indicated. Data were pooled from 24 cells for each condition. Note, MA and Baf-A1 treatment increased the number of larger diameter vacuoles, which was further enhanced by P2X4 expression. (D) Summary of percentage of vacuolated cells (with at least three vacuoles of >2 μm in diameter) from three independent experiments run in triplicates and >250 cells counted for each experiment. Coexpression of rP2X4-C353W diminished MA-induced vacuolation in cells expressing rP2X4-GFP. NT, not treated. (E) Cos1 cells expressing rP2X4-H286A-GFP showed enlarged vacuoles, which was not affected by MA. (F) Copper inhibited MA-induced vacuolation in Cos1 cells expressing rP2X4-GFP. Cells were pretreated with 20 μM CuSO₄ for 5 h at 37°C and then incubated with 10 mM MA for 1 h. (G) Incubation with Cu²⁺ (100 μM CuSO₄ overnight) reduced vacuole size in Cos1 cells expressing P2X4-H286A-GFP. (H) Summary of percentage of vacuolated cells expressing rP2X4-GFP or rP2X4-H286A-GFP illustrating the effects of MA and Baf-1 and the inhibition by Cu²⁺. Note, Cu²⁺ was coapplied with MA for the P2X4 group. Analyses were performed as described in D. (I) MA-induced vacuolation in cells expressing P2X4-H140A-GFP was unaffected by Cu²⁺ treatment. Quantification of vacuolated cells is shown on the right. Analyses were performed as described in D. (J) TEM images of Cos1 cells that expressed P2X4-GFP showing MA-induced vacuolation and its inhibition by Cu²⁺ and W7. (K) Quantification of the percentage of lysosomes with diameters <0.5 μm per TEM field. 10 randomly selected fields were counted each time, and each sample was counted at least three times from two randomly chosen TEM sample grids. Bars: (fluorescence images) 5 μm; (TEM images) 0.5 μm. Values are means ± SEM; *, P < 0.05; **, P < 0.01.

conditions (Fig. 1, E and H). Importantly, although MA and Baf-A1 significantly increased the vacuolation of cells expressing rP2X4-GFP (Fig. 1, D and H), they did not affect that of cells expressing rP2X4-H286A-GFP (Fig. 1, E and H).

Noticeably, weakly dextran-loaded vacuoles were also observed after MA and Baf-A1 treatment. These could be caused by heterotypic fusions of LEL with other organelles such as early endosomes. To test this possibility, cells were coexpressed with EEA1-GFP, an early endosome marker, and Lamp1-mCherry or P2X4-mCherry. MA significantly increased the size of Lamp1-positive and P2X4-positive vacuoles. However, MA did not increase the colocalization of EEA1 with either Lamp1 or P2X4 (Fig. S1, G and H). These data suggest that MA likely specifically facilitated P2X4-mediated LEL fusion (Bakker et al., 1997; Ward et al., 1997).

Previously, Cu^{2+} was shown to inhibit P2X4 activity (Coddou et al., 2003; van den Berghe et al., 2007). Preincubating for 5 h with 20 µM Cu^{2+} in culture medium substantially attenuated MA-induced vacuolation in rP2X4-GFP–expressing cells (Fig. 1, F and H). Consistently, 100 µM Cu^{2+} also markedly decreased the vacuolation of cells expressing P2X4-H286A-GFP (Fig. 1, G and H). Interestingly, vacuolation of cells expressing P2X4-H140A-GFP, a Cu^{2+}-insensitive P2X4 mutant (Fig. S2 C; Coddou et al., 2003), was unaffected by the Cu^{2+} treatment (Fig. 1 I). Collectively, these results argue for an important role of P2X4 channel activity in LEL vesicle trafficking and vacuole size control.

It has been suggested that increases in lysosomal pH induce lysosome exocytosis (Tapper and Sundler, 1995; Qureshi et al., 2007). As such, MA and Baf-A1 could indirectly cause vacuolation by increasing exocytotic insertion of P2X4 on the PM, which could be activated by ATP released to the extracellular space by the same exocytic event and in turn mediate Ca^{2+} influx to drive vesicle trafficking. To exclude this possibility, we treated cells with MA in a Ca^{2+}-free external solution and showed that the removal of extracellular Ca^{2+} did not alter the ability of MA to induce vacuolation (Fig. S1, I and J). These data suggest that the enlarged vacuoles in cells expressing rP2X4-GFP were unlikely caused by the activity of PM P2X4. Furthermore, MA did not induce significant lysosome exocytosis in Cos1 cells, as shown by the lack of an MA-evoked increase in the level of lysosomal enzyme β-hexosaminidase in the culture medium (Fig. S1 K). As a control, β-hexosaminidase level in the medium was significantly enhanced by the treatment of 1 µM ionomycin, a Ca^{2+} ionophore (Fig. S1 K).

An increase in enlarged vacuoles should be accompanied with a decrease in smaller vacuoles if the P2X4 activity was to promote LEL fusion rather than biogenesis. To test this, we measured diameters of vacuoles/LELs from images taken by transmission EM (TEM). We found that P2X4 expression resulted in a significant decrease in the percentage of small vacuoles/LELs (<0.5 µm in diameters) and MA treatment further decreased it (Fig. 1, J and K). Importantly, the reduction in the percentage of small vacuoles/LELs was rescued by coapplication of Cu^{2+} during the MA treatment. Moreover, MA treatment also caused a significant decrease in small LELs in WT control Cos1 cells, and the effect was abolished by the coapplication of Cu^{2+} (see Fig. 5, G and H). Therefore, concomitant with the increase in enlarged vacuoles as revealed by confocal and EM, P2X4 activation also resulted in a corresponding decrease in smaller vacuoles. To test whether P2X4 expression and activation of LEL P2X4 by MA and Baf-A1 had any effect on LEL biogenesis,

we measured Lamp1 expression levels in WT and rP2X4-GFP–expressing Cos1 cells with or without drug treatment. Western blotting showed no obvious differences in Lamp1 levels under all treatment conditions (Fig. S3). Collectively, our data suggest that P2X4 activation promotes LEL vacuole enlargement.

Ca^{2+} dependence on P2X4-mediated LEL vacuolation

Release of luminal Ca^{2+} from organelles is important in the regulation of many intracellular fusion/fission events, including the fusion of yeast vacuoles (Peters and Mayer, 1998), heterotypic fusion of late endosomes with lysosomes (Pryor et al., 2000), homotypic fusion of lysosomes (Bakker et al., 1997), and reformation of lysosomes from hybrid compartments (Pryor et al., 2000). As a nonselective cation channel, P2X4 mediates the release of Ca^{2+} or/and Na^+ from LEL lumen. We hypothesized that LEL Ca^{2+} release through P2X4 is the main mechanism that triggers vacuolation. To measure the Ca^{2+} permeability of the LEL P2X4 channel, enlarged LEL vacuoles from cells expressing rP2X4-GFP were used for whole-lysosome recording with a pipette solution that contained Ca^{2+} as the only cation, plus 0.1 mM ATP at pH 7.4 to stimulate P2X4 (Fig. 2 A). Large inward currents (mean current amplitude at −140 mV = 606 ± 136 pA, $n = 4$) were detected immediately after the formation of the whole-lysosome patch, which declined with time (Fig. 2 B), demonstrating the permeation of Ca^{2+} through LEL P2X4 channels.

To test whether or not intracellular Ca^{2+} elevation is required for LEL vacuolation, cells expressing rP2X4-GFP were preincubated for 0.5 h with 10 µM BAPTA-AM, a membrane-permeable Ca^{2+} chelator. This treatment dramatically decreased the effect of MA or Baf-A1 on vacuolation (Fig. 2, C and D). Together, these data support the view that LEL Ca^{2+} release through P2X4 is required for vacuolation.

To show that alkalization caused LEL Ca^{2+} mobilization via P2X4, we fused G-GECO, a single-wavelength genetically encoded Ca^{2+} indicator (Zhao et al., 2011), to the cytoplasmic C terminus of P2X4 and the dominant-negative P2X4-C353W (Fig. 2 E). Both constructs showed prominent colocalization with Lamp1 when expressed in Cos1 and HEK293T cells (Fig. 2 F). Because of the sensitivity of G-GECO to pH, these probes were not suitable to measure MA- or NH_4Cl^--induced Ca^{2+} transients. However, MA or NH_4Cl pretreatment dramatically decreased the fluorescence signal elicited by 200 µM glycyl-phenylalanine 2-naphthylamide (GPN), a substrate of the lysosomal exopeptidase cathepsin C that causes lysosomal membrane rupture and Ca^{2+} release (Cao et al., 2014), in cells that expressed P2X4-GECO (Fig. 2 G) but not P2X4-C353W-GECO (Fig. 2 H), suggesting that lysosomal Ca^{2+} content was reduced by P2X4 activation. The difference in GECO signal was not caused by GECO expression because the maximal fluorescence intensity induced by 1 µM ionomycin (in 2 mM Ca^{2+} external solution) was comparable between P2X4-GECO and P2X4-C353W-GECO (Fig. 2 I; Shen et al., 2012). Altogether, these data suggest that P2X4 functions as an LEL Ca^{2+} release channel.

Interaction of P2X4 and CaM in LELs

CaM is a Ca^{2+} sensor that has been suggested to mediate endosome/lysosome fusion in mammalian cells as well as the fusion of yeast vacuoles, the counterpart of mammalian lysosomes (Colombo et al., 1997; Peters and Mayer, 1998). CaM has also
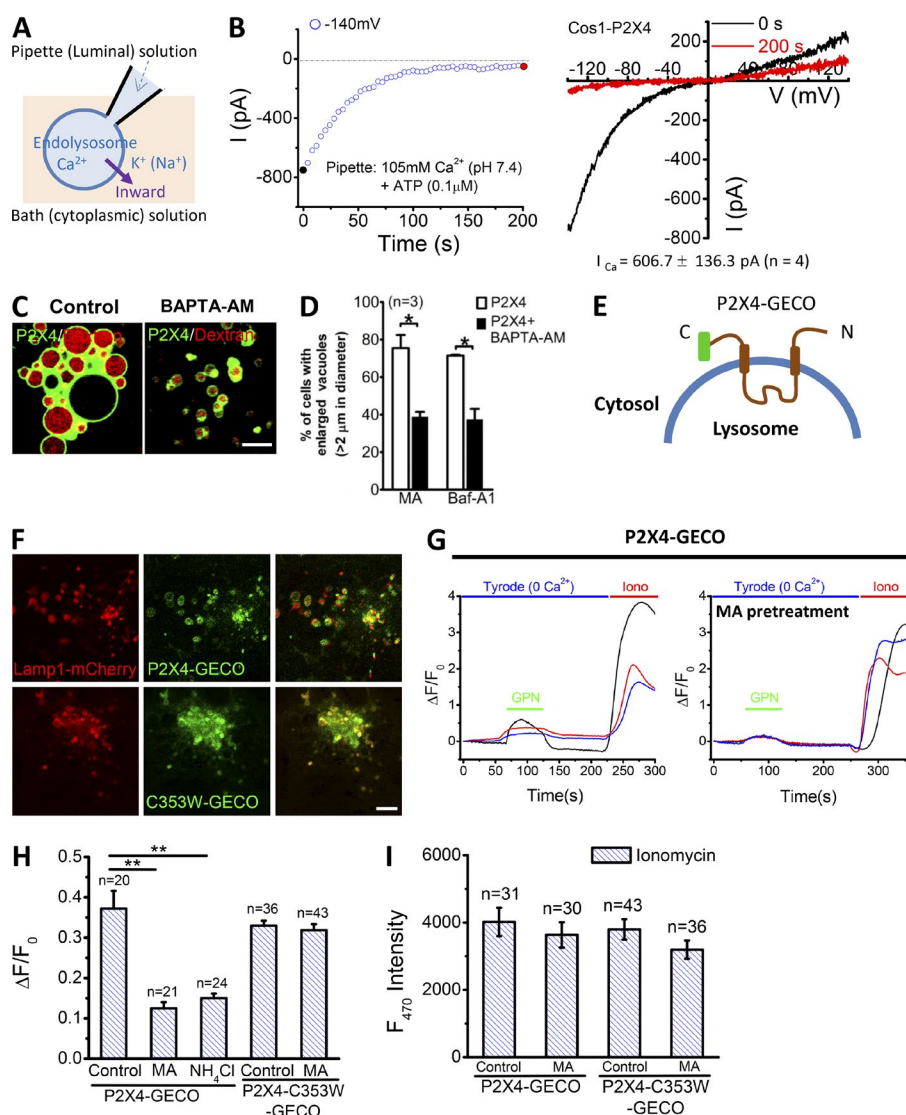
Figure 2. **P2X4-mediated LEL Ca²⁺ release was involved in alkalinization-induced vacuolation.** (A) Illustration of whole-lysosome recording configuration. Enlarged LELs were manually isolated from cells pretreated with 1 µM vacuolin-1 (>2 h). The pipette (luminal) solution contained 105 mM of isotonic Ca²⁺. The bath (cytoplasmic) solution was a K⁺-based internal solution. The inward current indicates cations flowing out of the LEL (arrow). (B) Ca²⁺ currents (inward) recorded from whole-lysosome patches using a pipette solution that contained Ca²⁺ as the sole cation, and 0.1 mM ATP with pH set to 7.4 to activate P2X4 from the vacuole expressing P2X4-GFP. (left) Time course of current at −140 mV with 0 representing the time of whole-lysosome patch formation; (right) current–voltage (I-V) relationship at the time points indicated. The mean maximal current amplitudes at −140 mV for four vacuoles are indicated at the bottom. (C) Preincubation with 10 µM BAPTA-AM (30 min at 37°C) suppressed the effect of MA on vacuolation in Cos1 cells expressing rP2X4-GFP. (D) Summary of vacuolated cells showing that BAPTA-AM pretreatment significantly blocked vacuolation induced by MA or Baf-A1. Values are means ± SEM; *, P < 0.05. (E) P2X4-GECO fusion strategy. GECO was fused to the C terminus of P2X4. (F) Colocalization of P2X4-GECO (top) or P2X4-C353W-GECO (bottom) with Lamp1-mCherry in Cos1 cells. (G) 10 mM MA (1 h) pretreatment of HEK293T cells that expressed P2X4-GECO significantly reduced 200 µM GPN-induced increase in GECO signal, indicating a loss of lysosomal Ca²⁺ content by MA. Representative GECO responses to GPN in three P2X4-GECO–expressing cells are shown for control (left) and MA treatment (right) groups. Iono, ionomycin. (H) Summary of peak GPN-induced increases in GECO fluorescence in cells that expressed P2X4-GECO or P2X4-C353W-GECO. Cells were pretreated or not treated with MA or NH₄Cl (both at 10 mM for 1 h) as indicated. The treatment solution was replaced with normal solution before GPN application. Numbers of cells tested are indicated in paren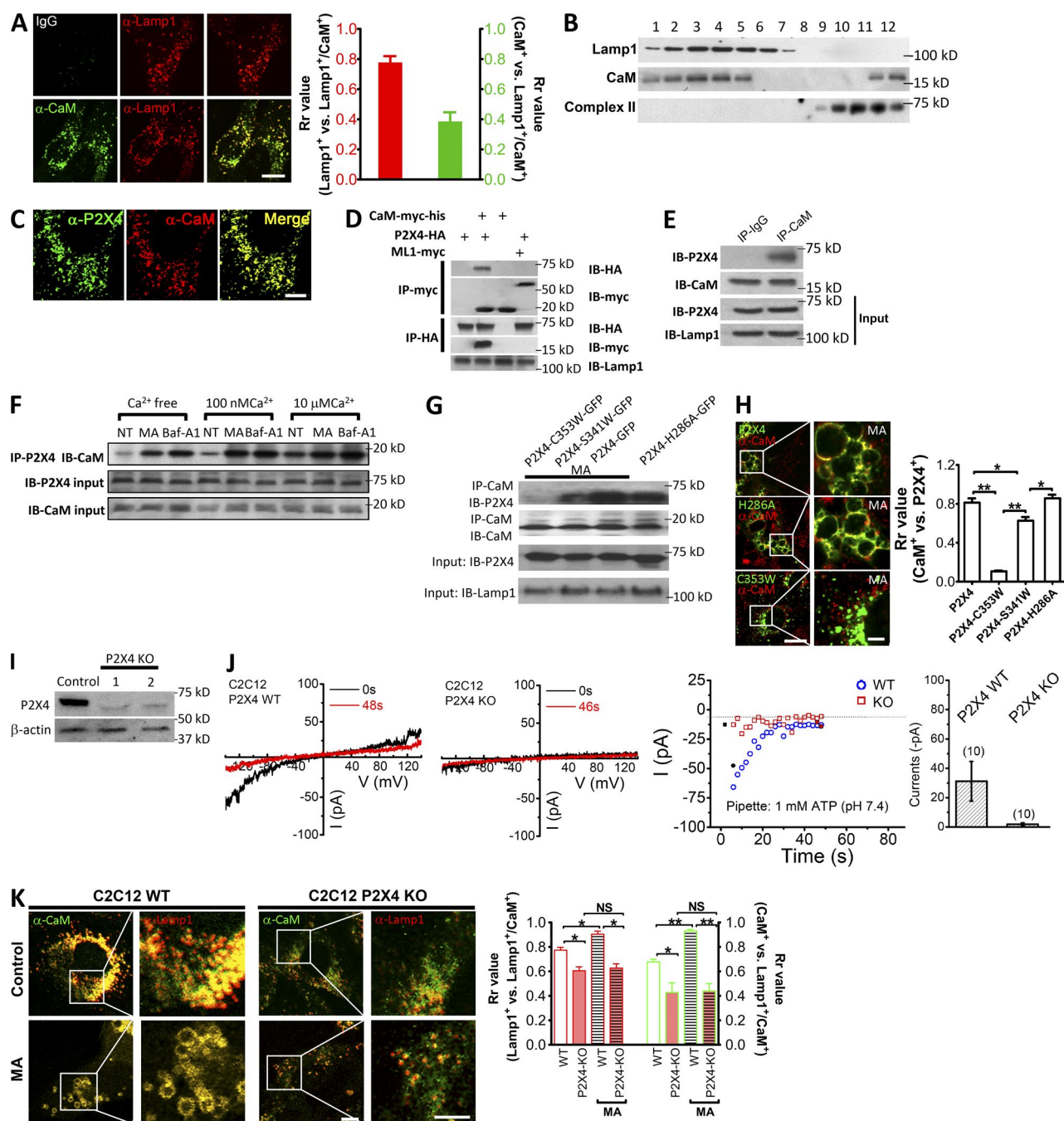theses. Note, MA did not deplete lysosomal Ca²⁺ in cells that expressed P2X4-C353W-GECO. Values are means ± SEM; *, P < 0.05, **, P < 0.01. (I) Comparable expression levels of P2X4-GECO and P2X4-C353W-GECO. Expression level of GECO was estimated by the maximal fluorescence signal induced by 1 µM ionomycin. Values are means ± SEM. Bars, 5 µm. F, fluorescence.

been shown to be associated with LEL membranes (Nielsen et al., 1987). We therefore hypothesized that the Ca²⁺-dependent LEL vacuolation might involve P2X4 interaction with CaM. To test this hypothesis, we first investigated the subcellular localization of CaM. A significant fraction of endogenous CaM was colocalized with Lamp1 in Cos1 cells by immunocytochemistry (Fig. 3 A). Most Lamp1-positive puncta contained CaM, and 32.7 ± 4.6% CaM-positive puncta was Lamp1 positive (n = 40 cells). By Western blotting, CaM was also found to be enriched in cellular fractions that contained LELs in samples from Cos1 cells prepared using density-gradient centrifugation (Fig. 3 B). Furthermore, by immunocytochemistry, we showed that endogenous CaM and P2X4 were well colocalized (Fig. 3 C).

The physical association between CaM and P2X4 was demonstrated by coimmunoprecipitation (co-IP) using Cos1 cells transfected with CaM-myc-his and rP2X4-HA (Fig. 3 D). As a control, TRPML1-myc did not coimmunoprecipitate P2X4-HA under the same experimental conditions (Fig. 3 D). Furthermore, endogenous P2X4 also coimmunoprecipitated with CaM from

purified Cos1 cell LEL fractions (Fig. 3 E). Therefore, P2X4 and CaM form a signaling complex at LEL membranes.

Interestingly, the association between P2X4 and CaM was Ca²⁺ dependent (Fig. 3 F), enhanced by either MA or Baf-A1 treatment (Fig. 3 F), and regulated by P2X4 activity (Fig. 3 G). Both the pH-insensitive P2X4 (H286A) mutant and MA-activated WT P2X4 associated more strongly with CaM than the nonfunctional S341W mutant. The dominant-negative C353W mutant inhibited the association. In agreement with the co-IP data, CaM was highly colocalized with P2X4 and P2X4-H286A but not P2X4-C353W (Fig. 3 H). To test the contribution of endogenous P2X4 to LEL localization of CaM, we knocked P2X4 out in C2C12 cells using the clustered regularly interspaced short palindromic repeat (CRISPR)–Cas9 system (Cong et al., 2013) with two separate targeting sequences. As shown in Fig. 3 I, both targeting constructs markedly reduced the expression of P2X4 as well as the ATP-evoked P2X4 currents (Fig. 3 J) and resulted in significant decreases in the colocalization of CaM with Lamp1 (Fig. 3 K). Consistent with data in Cos1

Figure 3. P2X4 activation recruited CaM to LEL membranes. (A) Immunocytochemistry of WT Cos1 cells stained with anti-CaM (or a control IgG) and anti-Lamp1. Most Lamp1-positive puncta contained CaM. Summary data collected from 40 cells are shown on the right; three independent experiments; means ± SEM. Bar, 10 µm. (B) Western blots showing the presence of CaM in Lamp1-containing LEL fractions (fractions 1–6). Note the presence of CaM (fractions 11 and 12) also in mitochondrial fractions as indicated by the presence of complex II. (C) Immunocytochemistry of WT Cos1 cells stained with anti-P2X4 and anti-CaM. CaM-positive puncta largely colocalized with P2X4-labeled organelles. Bar, 5 µm. (D) Co-IP of P2X4 and CaM. Cos1 cells were transiently transfected with CaM-myc-his, P2X4-HA, and TRPML1-myc (ML1-myc) alone or in combinations as indicated. After 24 h, LEL (fractions 1–6 as in B) were collected and lysed by adding 0.5% Triton X-100. Samples were immunoprecipitated with protein A/G–anti-myc and blotted with anti-HA and vice versa. The anti-myc Western (immunoblot [IB]-myc) in immunoprecipitation (IP)-myc samples and anti-HA Western (immunoblot-HA) in immunoprecipitation-HA samples showed similar levels of protein inputs in the immunoprecipitation assays. Anti-Lamp1 Western (immunoblot-Lamp1) was also used as a control for the amount of LELs subjected to immunoprecipitation. (E) Co-IP of endogenous CaM and P2X4 in Cos1 cell LEL fractions. IgG was used as a negative control. The lower blots show comparable inputs of P2X4 and Lamp1 in the LEL preparations. (F) Co-IP of P2X4 and CaM in isolated Cos1 cell LEL preparations with the immunoprecipitation buffer containing 0, 100 nM, or 10 µM free Ca²⁺ (buffered by EGTA). Samples from 10 mM MA (2 h)- and 200 nM Baf-A1 (2 h)–treated cells showed increased association between P2X4 and CaM. The presence of Ca²⁺ in the co-IP solution also enhanced the P2X4-CaM association. NT, not treated. (G) P2X4 activity enhanced association between P2X4 and CaM. P2X4-C353W-GFP had weak or no association with CaM even with MA treatment, whereas P2X4-H286A-GFP displayed strong association with CaM without MA treatment. Note, the dead but not dominant-negative P2X4-S341W-GFP associated with CaM probably because of the functionality of endogenous P2X4. (H) Colocalization of CaM with vacuoles that contained P2X4-GFP, P2X4-H286A-GFP, and P2X4-S341W-GFP but not those that had P2X4-C353W-GFP. Cells treated with MA are indicated. Summary data for colocalization coefficients (Rr) of GFP and CaM are shown on the right. (n = 52 cells, three independent experiments; means ±

cells, MA treatment increased CaM colocalization with Lamp1 and induced vacuolation in control C2C12 cells and both effects were abolished by P2X4 knockout (Fig. 3 K also see Fig. 5, E and F, for effect on vacuolation). Collectively, these data suggest that activation of P2X4 and the consequent Ca^{2+} release promote CaM association with P2X4.

CaM involvement in P2X4-mediated LEL trafficking

The Ca^{2+}-dependent physical association between P2X4 and CaM suggests that CaM may serve as a downstream sensor that promotes vacuolation in response to LEL Ca^{2+} release through P2X4. Supporting this idea, 10 µM W7, a CaM antagonist, inhibited vacuolation of P2X4-GFP–expressing cells induced by MA and Baf-A1 (Figs. 4 A and S1 C). W7 also abolished the effect of MA on reducing the percentage of small vacuoles (Fig. 1, J and K). Moreover, P2X4-mediated vacuole enlargement was enhanced by coexpression of WT CaM but suppressed by that of a dominant-negative CaM, CaM(1–4), which had all four Ca^{2+}-binding EF hands disrupted by mutations (Fig. 4 B; Xia et al., 1998). The suppression by CaM(1–4) was also prominent in the presence of MA or Baf-A1 (Fig. 4 B) and was clearly seen in cells that expressed P2X4-H286A-GFP (Fig. 4 C). In contrast, the P2X4-mediated vacuolation was not affected by expressing a dominant-negative construct of Syt VII (Tsuboi and Fukuda, 2007; Samie et al., 2013) or the knockout of ALG-2 (Fig. S4).

Our data thus suggest that among the three Ca^{2+}-binding proteins that have been proposed to regulate intracellular membrane trafficking, CaM is involved in Ca^{2+}-dependent LEL vacuolation. To further test whether P2X4 activation is absolutely required for this effect, we raised cytoplasmic Ca^{2+} using thapsigargin that releases endoplasmic reticulum Ca^{2+}. 0.4 µM thapsigargin (90 min) significantly increased the size of Lamp1-positive vacuoles in Cos1 cells. This effect was further enhanced by the expression of WT CaM but inhibited by CaM(1–4) (Fig. 4 D). To exclude the possibility that CaM regulated LEL P2X4 activity and then triggered vacuolation, P2X4 activity in enlarged LEL was recorded in the presence and absence of bath-applied Ca^{2+}/CaM. We found that Ca^{2+}/CaM had no effect on P2X4 currents (Fig. 4, E, F, and I). Similarly, CaM overexpression did not affect P2X4 current (Fig. 4, G–I). Altogether, these data further suggest that CaM acts purely as a Ca^{2+} sensor to induce vacuolation downstream of LEL P2X4.

Involvement of endogenous P2X4/CaM in LEL trafficking

To further investigate the role of P2X4/CaM in LEL trafficking, we measured the effect of MA on vacuole size in WT Cos1 cells. MA treatment led to vacuolation, which was inhibited by Cu^{2+}, BAPTA-AM, and W7 (Fig. 5, A and B), consistent with the idea that MA-induced vacuolation is dependent on Ca^{2+}/

CaM. Similar results were obtained with cells that expressed Lamp1-GFP (Fig. 5 B). To test the involvement of endogenous P2X4, we expressed the dominant-negative rP2X4-C353W-GFP in Cos1 cells and showed that it suppressed the MA-induced vacuolation (Fig. 5, C and D). Likewise, the expression of rP2X4-C353W-GFP also dramatically reduced the ability of Baf-A1 to induce the vacuolation (Fig. 5 D). Between control and P2X4 knockout C2C12 cells (as in Fig. 3, I–K), although no obvious difference in the vacuole size was observed under untreated conditions, the MA-induced vacuolation was markedly suppressed by the knockout of P2X4 (Fig. 5, E and F). These data, therefore, clearly established the contribution of endogenous P2X4 in vacuolation induced by MA and Baf-A1.

Similar to cells expressing P2X4-GFP, MA treatment decreased the percentage of small vacuoles/LELs in WT Cos1 cells, as revealed in TEM images, and this was inhibited by Cu^{2+} and W7 treatment (Fig. 5, G and H). Expression of P2X4-C353W-GFP mutant also inhibited this effect (Fig. 5 I). Similar negative results were obtained in P2X4 knockout C2C12 cells, although MA treatment reduced small vacuoles/LELs in control C2C12 cells (Fig. 5, J and K). Importantly, none of the treatments, MA, W7, Cu^{2+}, P2X4-C353W-GFP expression, and P2X4 deficiency, altered LEL biogenesis (Fig. S3). Collectively, our data strongly support the roles of P2X4/CaM in LEL vacuolation.

Direct observation of P2X4-mediated LEL fusion events

To directly measure membrane fusion, rP2X4-GFP–expressing cells loaded with dextran were monitored using time-lapse live cell imaging, and fusion events were quantified. Fig. 6 A shows an example in which two vacuoles expressing rP2X4-GFP fused with each other and formed a larger vacuole in the presence of MA. Quantification of fusion events indicated that MA treatment dramatically increased fusion by 5.65-fold, and this was suppressed by Cu^{2+}, BAPTA-AM, and W7 treatment (Fig. 6 B). In accordance with these results, the activation of endogenous P2X4 also increased fusion events by 6.15-fold, and this was suppressed by Cu^{2+}, BAPTA-AM, W7, or expression of P2X4-C353W-GFP (Fig. 6, C and D). Our live cell imaging data thus suggest that the P2X4/CaM-mediated vacuolation is likely caused by an enhancement on membrane fusion.

To confirm that the P2X4/CaM coupling promotes LEL fusion, we adopted an in vitro fusion assay (Brandhorst et al., 2006; Moreau et al., 2011). Postnuclear fractions (PNFs) isolated from cells expressing P2X4-GFP and P2X4-DsRed (or mCherry) were mixed together and seeded in an observation chamber, untreated or treated with MA or Baf-A1. PNFs isolated from cells expressing Lamp1-GFP and Lamp1-mCherry were used as controls. From confocal images, the colocalization of GFP and DsRed (or mCherry) was determined by Pearson's colocalization coefficient (Rr) and used as an indicator

SEM; *, P < 0.05; **, P < 0.01 by analysis of variance.) These data suggest that activation of P2X4 recruits CaM to P2X4-containing LEL vacuoles. Bars: (left) 10 µm; (right) 2 µm. (I) Western blot showing expression of endogenous P2X4 in control (vector transfected) C2C12 cells and cells with the gene for P2X4 knocked out (KO) using the CRISPR-Cas9 system. Two guide DNA constructs (1 and 2) with independent targets on the P2X4 gene were used to exclude potential off-targeting effects. The faint P2X4 bands detected in P2X4 knockout cell lysates probably represent a small amount of residual proteins from either transfected or nontransfected cells. (J) 1 mM ATP evoked currents in whole-lysosome patches for WT and P2X4 knockout C2C12 cells. Pipette solution had pH 7.4. I-V curves for indicated time points after whole-lysosome formation, and time courses for currents at −140 mV are shown. The dotted line indicates 0 pA. Peak current amplitudes at −140 mV are summarized on the right. (K) P2X4 deficiency resulted in decreased colocalization of CaM with Lamp1 in C2C12 cells. Immunocytochemistry images are shown on the left. Cells were either treated with MA or not treated. Summary data for Rr between CaM and Lamp1 are show on the right. (n > 28 cells for each condition, three independent experiments; means ± SEM; *, P < 0.05; **, P < 0.01 by analysis of variance.) Bars: (whole-cell images) 5 µm; (magnifications) 3 µm.
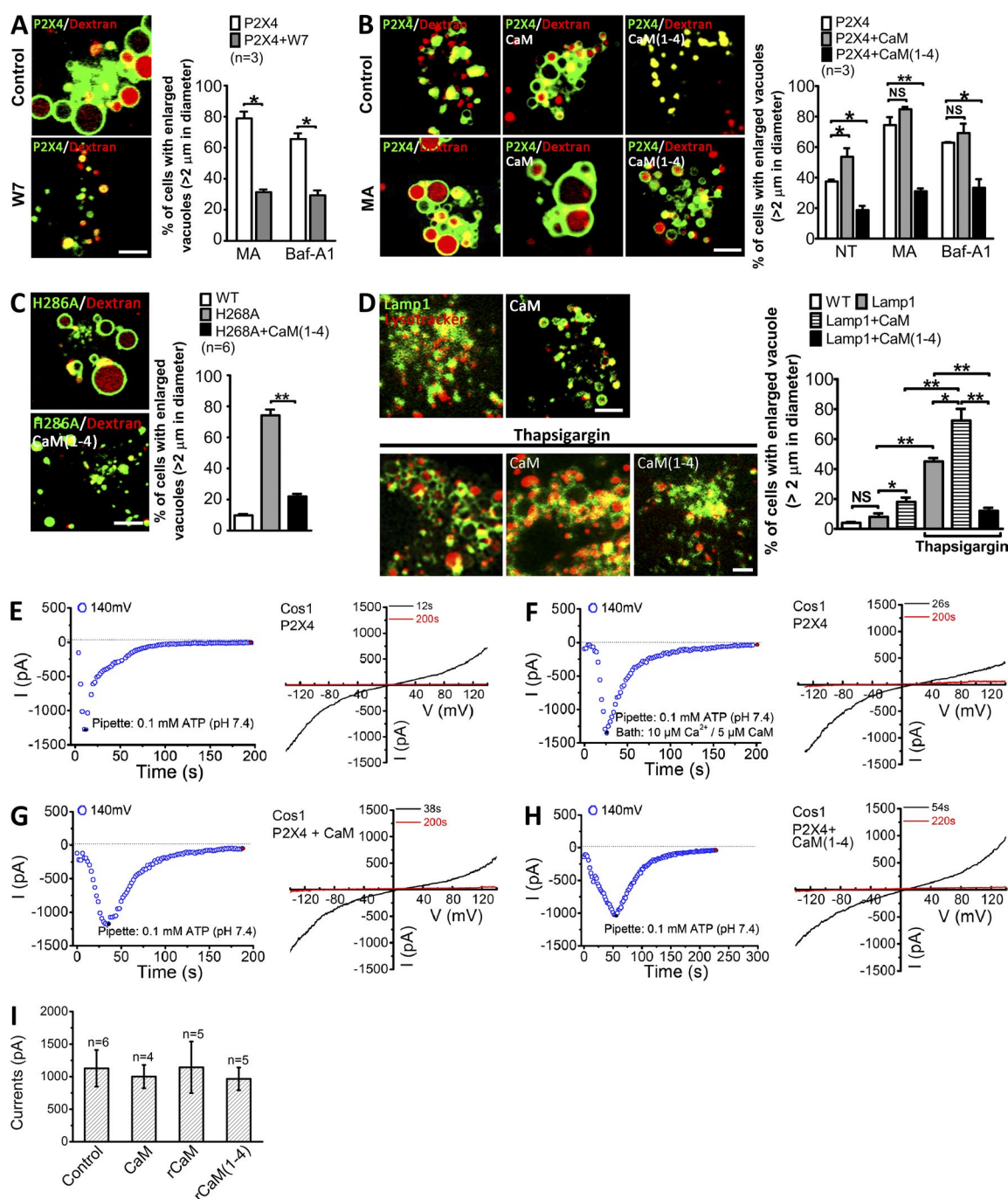
Figure 4. **CaM was involved in P2X4-mediated vacuolation.** (A) A CaM inhibitor, 10 µM W7 (1 h) significantly suppressed MA-induced vacuolation in Cos1 cells expressing rP2X4-GFP. Summary of vacuolated cells is shown on the right. Vacuolation was induced by either MA or Baf A1 as indicated. (B) Vacuolation of rP2X4-GFP expressing Cos1 cells was enhanced by coexpression of WT CaM but suppressed by that of CaM(1–4), a dominant-negative CaM mutant. Bar graph at right shows percentage of vacuolated cells under conditions indicated. (C) Coexpression of CaM(1–4) dramatically reduced vacuolation in Cos1 cells that expressed rP2X4-H286A-GFP. The bar graph on the right shows the percentage of vacuolated cells in untransfected (WT) and rP2X4-H286A-GFP–transfected Cos1 cells without or with CaM(1–4). (D) Vacuolation in Cos1 cells that expressed Lamp1-GFP without or with WT CaM or CaM(1–4). 0.4 µM thapsigargin (90 min) was applied as indicated. Thapsigargin increase vacuolation, which was enhanced by CaM but suppressed by CaM(1–4). Summary of vacuolated cells under the indicated conditions is shown on the right. Bars, 5 µm. (E–I) CaM did not alter P2X4 currents in whole-lysosome patches. Enlarged vacuoles were obtained from cells that expressed P2X4-GFP (E and F), P2X4-GFP + CaM (G), and P2X4-GFP + CaM(1–4) (H) and recorded using a pipette solution that contained 0.1 mM ATP with pH set at 7.4, without (E, G, and H) or with 10 µM Ca^{2+} and 5 µM CaM (F). Left graphs show current development at −140 mV after the formation of whole-lysosome configuration; right graphs show I-V curves of currents at the indicated time points. (I) Summary of peak currents at −140 mV. All cells expressed P2X4-GFP. CaM: addition of purified CaM in the bath; rCaM and rCaM(1–4): cotransfection of rat CaM constructs. Values are means ± SEM; *, P < 0.05; **, P < 0.01.
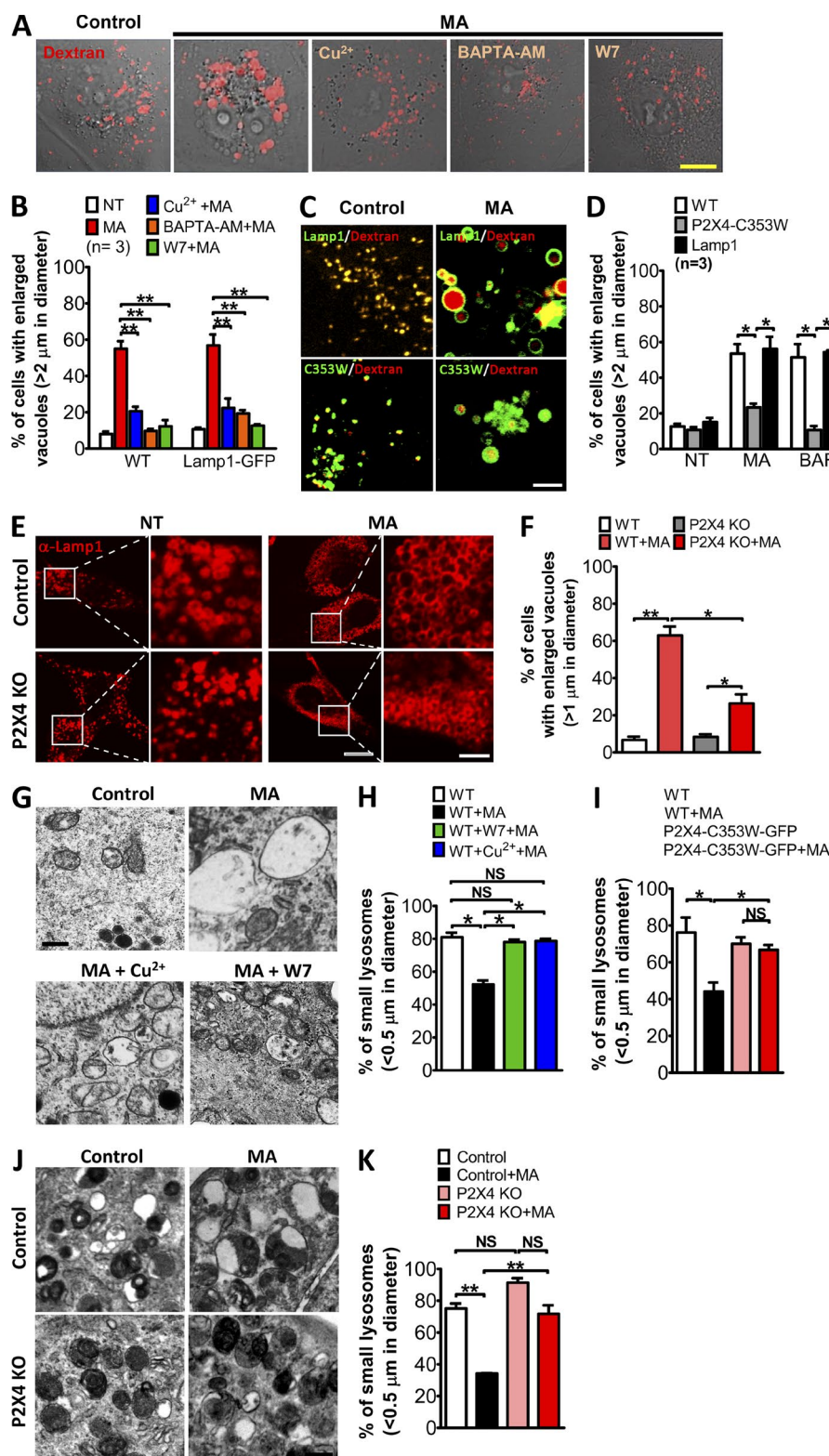
Figure 5. **Activation of endogenous P2X4 induced vacuolation in a Ca^{2+}/CaM-dependent manner.** (A) MA-induced vacuole enlargement in Cos1 cells loaded with Texas red 10-kD dextran was inhibited by pretreatment with 20 μM CuSO$_4$, 10 μM BAPTA-AM, or 3 μM W7. Bar, 10 μm. (B) Percentage of vacuolated cells in WT or Lamp1-GFP–expressing Cos1 cells under indicated conditions. NT, not treated. (C) Expression of P2X4-C353W-GFP suppressed MA-induced vacuolation in Cos1 cells. Lamp1-GFP–expressing cells were used as controls. Bar, 5 μm. (D) Percentage of vacuolated cells induced by MA or Baf-A1 in WT Cos1 cells and cells that expressed P2X4-C353W-GFP or Lamp1-GFP. (E and F) P2X4 knockout in C2C12 cells suppressed MA-induced vacuolation. WT and P2X4 knockout C2C12 cells were treated with 10 mM MA for 3 h, and cells were fixed and stained for Lamp1. Shown are representative images (E) and statistics for cells that contained vacuoles with diameters >1 μm (F). Bars: (whole-cell images) 10 μm; (magnifications) 3 μm. (G–J) Representative TEM images (left) and statistics of LELs with diameters <0.5 μm (right) for WT Cos1 cells (G) untransfected (WT) and P2X4-C353W-GFP–transfected Cos1 cells (I) and control (vector transfected) and P2X4 knockout (KO) C2C12 cells (J) untreated or treated with MA. Note the large vacuoles and scarcity of smaller LELs in MA-treated cells. Cu^{2+} and W7 (all conditions are the same as in A) prevented MA induced reduction of smaller LELs (G). Expression of P2X4-C353W-GFP (I) and P2X4 knockout (J and K) also suppressed the MA effect. For quantification, LELs in 10 randomly selected fields were counted each time, and each sample was counted at least three times from four randomly chosen TEM sample grids. Bars, 0.5 μm. Quantification data in A–K. Values are means ± SEM; *, P < 0.05; **, P < 0.01.

of fusion (Rong et al., 2012). The fusion rate was dependent on LEL density and incubation time (Fig. S5). We used the high density and 60-min incubation time for quantification. As expected for P2X4/CaM to promote fusion, the colocalization between P2X4-GFP and P2X4-DsRed was better than that between Lamp1-GFP and Lamp1-mCherry (Fig. 7, A–D); treatment with MA and Baf-A1 increased the colocalization for both

P2X4 pairs and Lamp1 pairs, and these effects were abolished by coapplication of Cu^{2+}, BAPTA, and W7 (Fig. 7, A–D). The results from the in vitro fusion assay support the role of P2X4 in LEL fusion and the involvement of Ca^{2+}/CaM in this process.

To investigate whether endogenous P2X4 is required for LEL fusion in the in vitro assay, Lamp1-GFP and Lamp1-mCherry were coexpressed with the dominant-negative rP2X4-
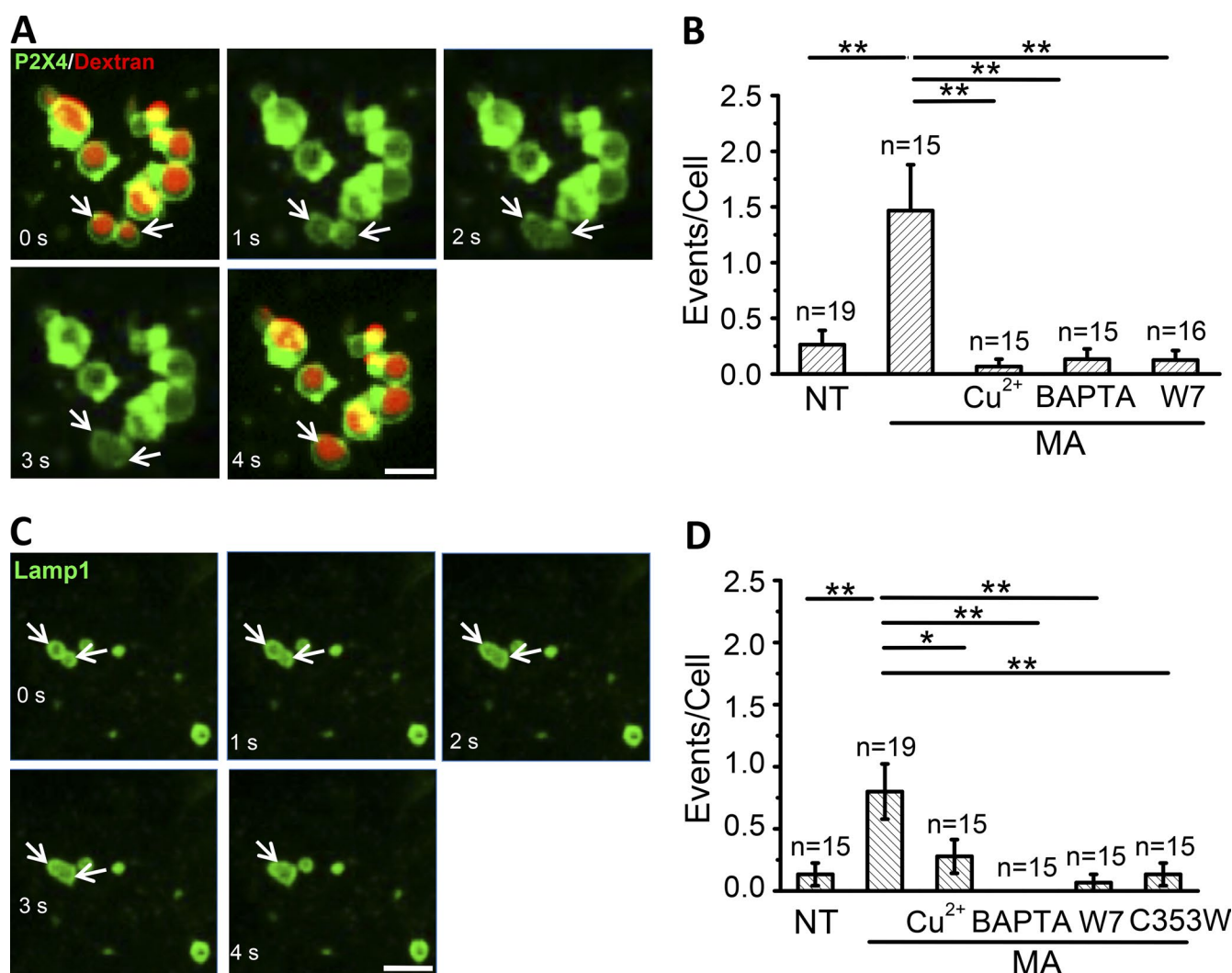
Figure 6. **Activation of P2X4 induced LEL membrane fusion in vivo in a Ca²⁺/CaM-dependent manner.** (A) Live cell time-lapse images showing the fusion of two Texas red dextran-loaded vacuoles (arrows) in cells expressing rP2X4-GFP after MA treatment. (B) Quantification of fusion events per cell within 45 min under indicated conditions monitored by live imaging in Cos1 cells expressing rP2X4-GFP. (C) Live cell imaging showing the fusion of two LELs (arrows) in Cos1 cells expressing Lamp1-GFP. (D) Quantification of fusion events per cell under indicated conditions monitored by live imaging in Cos1 cells expressing Lamp1-GFP. Number of cells recorded was indicated on top of each bar. Experiments were repeated three times independently. Note, the number of fusion events was increased by MA, which was inhibited by Cu²⁺, BAPTA-AM, W7, or expression of P2X4-C353W. (B and D) Values are means ± SEM; *, $P < 0.05$; **, $P < 0.01$. Bars, 5 μm. NT, not treated.

C353W in Cos1 cells before PNF preparation. The expression of rP2X4-C353W dramatically decreased the colocalization between Lamp1-GFP and Lamp1-mCherry in MA-treated samples (Fig. 7 E). Moreover, colocalization between Lamp1-GFP and Lamp1-mCherry in PNF prepared from separately transfected C2C12 cells was also significantly enhanced by the treatment with MA and Baf-A1, and these effects were abolished by the knockout of P2X4 (Fig. 7 F). Collectively, our data clearly demonstrate that P2X4 activation promotes LEL fusion, acting via the Ca²⁺–CaM pathway.

Discussion

Lysosomes are dynamic organelles that continuously fuse with themselves and with other organelles during processes of endocytosis, phagocytosis, autophagy, and membrane repair. Dysfunction of lysosomes has been implicated in lysosomal

storage diseases, cancer, neurodegenerative disorders, and aging-related diseases. It is therefore important to understand the mechanisms involved. Although Ca²⁺ released from LEL is thought to be critical for fusion, the molecular identities of the Ca²⁺ release channel and the Ca²⁺ sensors remained unclear. Recently, intracellular P2X channels have been shown to be important for vesicle fusion with the PM in *Dictyostelium discoideum* and for the dilation of vesicle/PM fusion pores in alveolar type II epithelial cells (Miklavc et al., 2011; Parkinson et al., 2014). Here, we demonstrate that mammalian P2X4 functions as an LEL Ca²⁺ release channel that plays a crucial role in vesicle fusion. We show that P2X4 activation promotes LEL fusion in a manner that depends on a rise in cytosolic Ca²⁺ and activation of CaM, which forms a signaling complex with P2X4 at LEL membranes. Whereas up-regulation of LEL P2X4/CaM by overexpressing exogenous P2X4/CaM or LEL alkalization promotes LEL fusion, down-regulation of P2X4/CaM through dominant-negative P2X4/CaM, P2X4 inhibition
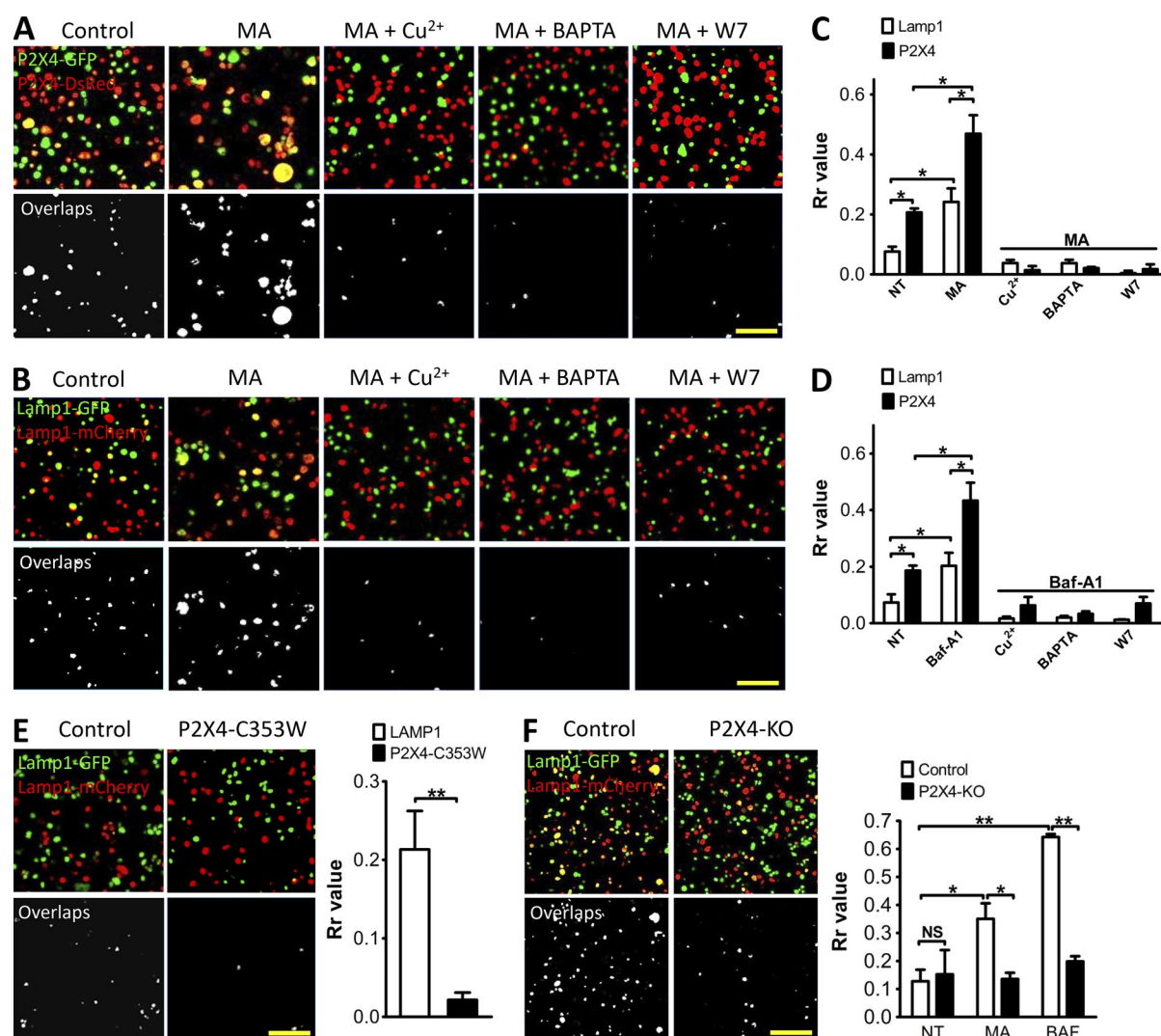
Figure 7. **Activation of P2X4–CaM pathway induced LEL fusion in a cell-free system.** (A) LELs isolated from Cos1 cells expressing P2X4-GFP and P2X4-DsRed individually were mixed to view the fusion in vitro. MA dramatically increased LEL fusion, which was inhibited by the addition of 20 µM Cu^{2+}, 10 µM BAPTA, and 3 µM W7 in the incubation solution. (B) Similar to A but LELs were isolated from Cos1 cells expressing Lamp1-GFP and Lamp1-mCherry individually. (C) Fluorescence-labeled LEL as shown in A and B were analyzed for Pearson's colocalization coefficient (Rr). A larger Rr indicates more colocalization/fusion. LEL expressing P2X4 showed significantly more fusion than those from cells that expressed the Lamp1-GFP/Lamp1-mCherry, which were further increased by MA. Cu^{2+}, BAPTA, and W7 inhibited MA-induced LEL fusion. (D) Baf-A1 increased P2X4-mediated fusion, which was also suppressed by Cu^{2+}, BAPTA, and W7. (E) LEL from Cos1 cells that expressed dominant-negative P2X4-C353W showed reduced colocalization, suggesting that inhibition of endogenous P2X4 decreased LEL fusion. (F) In C2C12 cells, P2X4 knockout reduced MA- and Baf-A1–induced fusion between LEL that contained Lamp1-GFP and that contained Lamp1-mCherry in the in vitro assay, supporting the critical role of P2X4 in LEL fusion. Values are means ± SEM from three independent experiments for C–F; *, P < 0.05; **, P < 0.01. Bars: (A and C) 10 µm; (E and F) 15 µm. KO, knockout; NT, not treated.

by Cu^{2+}, CRISPR-Cas9–based P2X4 knockout, or inhibition of CaM by W7 suppresses LEL fusion.

One important question is how the P2X4-mediated fusion process is regulated if LEL P2X4 is constantly exposed to its agonist, ATP. Recently, we demonstrated that LEL P2X4 is tightly regulated by luminal pH. The channel is minimally activated under the normal acidic LEL luminal pH, but alkalization of the luminal pH dramatically increases its activity (Huang et al., 2014). We therefore propose that pH regulation of P2X4 provides a mechanism to modulate LEL fusion. In support of this, we found that activation of LEL P2X4 by alkalization promoted LEL fusion and vacuolation. Our data are consistent with the findings that the proton pump activity of V-ATPase is not required for LEL fusion (Baars et al., 2007; Peri and Nüsslein-Volhard, 2008).

It has been suggested that luminal Ca^{2+} release is essential for the fusion of intracellular organelles (Pryor et al., 2000; Morgan et al., 2011). Our data suggest that P2X4 fulfills the function of mediating Ca^{2+} efflux from LEL lumen. Consistent with the cytoplasmic side of action for Ca^{2+} on fusion, chelating cytosolic Ca^{2+} inhibited vacuolation mediated by P2X4. Therefore, a Ca^{2+} sensor localized at the cytoplasmic side of LEL membranes is required. Among the three Ca^{2+}-sensitive proteins that have been shown to be associated with LEL, CaM (Colombo et al., 1997; Peters and Mayer, 1998), Syt VII (Martinez et al., 2000), and ALG-2 (Vergarajauregui et al., 2009), we found CaM to be physically associated with P2X4 and play a critical role in P2X4-mediated vacuolation and LEL fusion. In fact, the association of CaM with LEL was at least partially dependent on P2X4 function. The presence of the Ca^{2+} release

channel and the Ca^{2+} sensor in the same complex implies a high efficiency of functional coupling between the two proteins. Consistent with its role in membrane fusion, CaM has been shown to interact with several SNARE proteins in a Ca^{2+}-dependent manner (Quetglas et al., 2000) and several SNARE proteins, such as VAMP-7, VAMP-8, and Syntaxin-7, have been implicated in LEL fusion (Luzio et al., 2007b).

Two other LEL Ca^{2+} release channels, TRPML1 and TPC2, have also been suggested to be involved in LEL fusion and/or fission (Cheng et al., 2010; Dong et al., 2010). However, mounting evidence supports the role of TRPML1 in fission but not fusion. First, TRPML1-null mutant cells display enlarged LELs and fission/retrograde trafficking defects (Chen et al., 1998; Treusch et al., 2004; Cheng et al., 2010). Second, an increase in LEL PI(3,5)P2, an endogenous agonist of TRPML1, leads to vacuole (LEL) fission/fragmentation in yeast (Efe et al., 2005), whereas the deficiency in PI(3,5)P2 causes vacuole enlargement in both yeast (Rudge et al., 2004; Efe et al., 2005) and mammalian cells (Dong et al., 2010). Third, studies have shown that the pump activity of V-ATPase is not required for fusion but is required for fission, and V-ATPase mutant cells display enlarged vacuoles (Baars et al., 2007; Peri and Nüsslein-Volhard, 2008). This phenocopies the morphological defect of TRPML1-null mutant cells and supports the idea that enlarged vacuole sizes reflects a defect in fission. Alternatively, it can also be explained based on the assumption that V-ATPase mutations disrupt the balance between fusion and fission mediated by P2X4 and TRPML1, respectively. Ironically, although P2X4 activity is suppressed by the low LEL pH, TRPML1 is enhanced by it. Therefore, the elevation of LEL pH resulting from V-ATPase mutations should facilitate P2X4-mediated fusion but suppress TRPML1-mediated fission. The size of LEL is controlled by a balance between fusion and fission.

Between TPC1 and TPC2, TPC2 is mainly LEL localized (Calcraft et al., 2009; Ogunbayo et al., 2015). Although two-pore channels have been implicated in vesicle trafficking (Ruas et al., 2010; Grimm et al., 2014; Lin-Moshier et al., 2014), whether they conduct sufficient Ca^{2+} current remains a controversy (Schieder et al., 2010; Wang et al., 2012). If Na^+ efflux is the main function of two-pore channels, the released Na^+ could reverse the charge repulsion that prevent docking and fusion of organelles (Wang et al., 2012). This would explain the observed vesicle aggregation in *Xenopus laevis* oocytes that overexpressed TPC2 (Lin-Moshier et al., 2014). However, like TRPML1, TPC2 is activated by PI(3,5)P2 and when luminal pH is acidic (Wang et al., 2012), which contrasts the role of PI(3,5)P2 in fission and the effect of alkalinization on fusion. Therefore, whether and how TPC2 contributes to LEL fusion remain to be elucidated.

Because both TRPML1 and P2X4 are Ca^{2+}-permeable channels, how LELs differentiate the two Ca^{2+} release processes and respond with opposite consequences remains a fascinating question. Because TRPML1 is inhibited by alkaline pH (Dong et al., 2008), whereas P2X4 is suppressed by acidic pH (Clarke et al., 2000), conditions that favor their activation are distinct. Possibly segregated subdomains responsible for fusion and fission exist on the LEL membrane with P2X4 enriched in the fusion domain and TRPML1 enriched in the fission domain. For fission or reformation, V-ATPase may be recruited to the fission domain, causing a decrease of the local pH, which in turn enhances Ca^{2+} release through TRPML1 to trigger fission. For fusion, the V-ATPase may be removed from the fusion domain, leading to an increase of the local pH and a consequent acti-

vation of P2X4, which signals through CaM to initiate fusion. Second, the fission and fusion machineries may use different Ca^{2+} sensors. We have demonstrated the unique involvement of CaM but not Syt VII and ALG-2 in P2X4-mediated fusion. It remains to be determined what the specific Ca^{2+} sensors are for TRPML1-mediated fission. A plausible candidate is ALG-2, which binds to TRPML1 and regulates its effect on endosome trafficking (Vergarajauregui et al., 2009). However, whether and how ALG-2 promotes LEL fission need further investigation.

Materials and methods

Cell culture
Cos1, C2C12, and HEK293T cells were obtained from ATCC and maintained in DMEM: Nutrient Mixture F-12 (DMEM/F12) supplemented with 10% fetal bovine serum (Invitrogen). Cells were cultured at 37°C in a 5% CO_2 atmosphere. For some experiments, cells were seeded on 0.1% poly-lysine–coated coverslips and cultured for 24 h before further experiments. Cells from passage numbers 5–25 were used for subsequent assays.

Antibodies and reagents
The following primary antibodies were used in immunofluorescent staining: rabbit anti-P2X4 (1:200; Alomone Labs), anti-Lamp1 (1:250; mouse anti–human [H4A3] and rat anti–mouse [1D4B]; Developmental Studies Hybridoma Bank), and mouse anti-CaM (1:200; Molecular Probes). Antibodies used for Western blotting were anti-Lamp1 (1:2,000; H4A3 and 1D4B), rabbit anti-P2X4 (1:2,000), mouse anti–Complex II (1:2,000; Invitrogen), mouse anti-GAPDH (1:5,000; Santa Cruz Biotechnology, Inc.), mouse anti-c-Myc (1:2,000; Santa Cruz Biotechnology, Inc.), rabbit anti-HA (1:2,000; Santa Cruz Biotechnology, Inc.), and rabbit anti-ALG2 (1:2,000; Thermo Fisher Scientific). HRP-conjugated goat anti–rabbit and goat anti–mouse antibodies were purchased from Thermo Fisher Scientific and Bio-Rad Laboratories, Inc. and used at 1:5,000 and 1:10,000 dilutions, respectively. Alexa Fluor 594 goat anti–rabbit antibody, Alexa Fluor 488 goat anti–rat antibody, fluorescein goat anti–mouse, and Texas red goat anti–mouse antibodies were from Invitrogen and were used at 1:250 dilution.

LysoTracker DND-99 red (50 nM; Invitrogen) and Texas red 10-kD dextran (1 mg/ml; Invitrogen) were used to label LELs. The following chemicals were used in the present study: 10 mM MA (pH adjusted to 7.4 with HCl; Sigma-Aldrich), 200 nM Bafilomycin A1 (Tocris Bioscience), 200 µM GPN (Santa Cruz Biotechnology, Inc.), 10 µM W7 (Sigma-Aldrich), 10 µM BAPTA and BAPTA-AM (Invitrogen), $CuSO_4 \cdot 5H_2O$ (10, 20, 50, or 100 µM; Sigma-Aldrich), 10 mM NH_4Cl (Sigma-Aldrich), 0.4 µM thapsigargin (Tocris Bioscience), and 1 µM ionomycin (Cayman Chemical).

Immunocytochemistry
Cells grown on coverslips were washed with PBS twice and fixed in 4% paraformaldehyde in PBS for 15 min at room temperature. Fixed cells were permeabilized with 0.1% Triton X-100 in PBS for 5 min and then blocked with 3% BSA in PBS for 60 min at room temperature. After three washes with PBS, cells were incubated with specific primary antibodies at 4°C overnight. After three times washing with PBS, cells were incubated with fluorescence conjugated secondary antibodies for 45 min at room temperature in the dark.

Confocal microscopy
Confocal fluorescent images were taken using an inverted confocal microscope (LSM 510 Axiovert 200M; Carl Zeiss) with a 63× oil-im-

mersion objective at room temperature. Sequential excitation wavelengths at 488 and 543 nm were provided by argon and helium-neon gas lasers, respectively. Emission filters BP515-565 and LP590 were used for collecting green and red images in channels one and two, respectively. After sequential excitation, green and red fluorescent images of the same cell were saved with ZEN2012 software (Carl Zeiss). Images were analyzed by software. The term colocalization refers to the coincident detection of above-background green and red fluorescent signals in the same region. Colocalization was analyzed using ImageJ (National Institutes of Health), and the Pearson's colocalization coefficient (Rr) was used as an indicator of fusion (Rong et al., 2012). 0 < Rf < 1 indicates vesicle fusion; −1 < Rr < 0 indicates that vesicles repel each other; Rr = 0 indicates a random scatter. The image size was set at 1,024 × 1,024 pixels.

Live imaging
Live imaging was performed on the EasyRatioPro system (Photon Technology International) with a heated stage. Intervals between the frames were set as 1 s. Lenses used were 40× on the EasyRatioPro system.

Molecular biology and biochemistry
Rat P2X4 receptor with enhanced GFP fused to the C terminus (rP2X4-GFP), C353W-GFP, and S341W-GFP were made as described previously (Qureshi et al., 2007). In brief, for rP2X4-GFP, the rat P2X4 cDNA was amplified by polymerase chain reaction using oligonucleotide primers to introduce a Kozak initiation sequence, remove the stop codon, and introduce NheI and SacII sites at the 5′ and 3′ ends, respectively. Amplification products were then cloned into the pEGFP-N1 vector (Addgene). Transgene length is 1,164 bp. The C353W, S341W, and H286A point mutations were made using site-directed mutagenesis kit (QIAGEN). The sequences of all amplified regions were verified using automated DNA sequencing (GENEWIZ). Plasmids rCaM-myc-his and its mutant are generous gifts from L. Mei (Georgia Regents University, Augusta, GA). In brief, the cDNA for rat CaM (450 bp) was cloned into pcDNA3.1/myc-his vector with a T7 promoter. Cloning sites are BamH1 and Kpn1 at the 5′ and 3′ ends. The plasmid of dominant-negative pShooter-Flag-Syt-VII-D172N/D303N-GFP was generously provided by M. Fukuda (Tohoku University, Miyagi Prefecture, Japan). Mouse Syt VII cDNA (1,209 bps) was cloned into pShooter-Flag-GFP vector with a cytomegalovirus promoter. Cloning sites are Nod1 at both 5′ and 3′ ends. The dominant-negative form was generated by introducing D172N and D303N point mutations. G-GECO construct was provided by R. Campbell (University of Alberta, Edmonton, Alberta, Canada) The P2X4-GECO and P2X4-C353W-GECO constructs were made by inserting the full-length GECO sequence (Zhao et al., 2011) between the HindIII and BamHI sites of a pcDNA6 plasmid that contains the rat P2X4 cDNA at the XhoI site. All constructs were confirmed by sequencing analysis, and protein expression was verified by Western blotting. Cos1 cells were transiently transfected using Lipofectamine 2000 (Invitrogen), and C2C12 cells were transfected using Neon electroporation system. Both methods reached >80% transfection efficiency.

P2X4-GECO Ca²⁺ imaging
Cells were trypsinized and plated onto glass coverslips 18–24 h after transfection with the P2X4-GECO constructs. The fluorescence intensity at 470 nm (F_{470}) was monitored using the EasyRatioPro system. LEL Ca²⁺ release was measured in a low external Ca²⁺ bath solution, which contained 145 mM NaCl, 5 mM KCl, 3 mM MgCl₂, 10 mM glucose, 1 mM EGTA, and 20 mM Hepes, pH 7.4. Ca²⁺ concentration in the nominally free Ca²⁺ solution is estimated to be 1–10 µM. With 1

mM EGTA, the free Ca²⁺ concentration in the low external Ca²⁺ bath solution is estimated to be <10 nM based on the MaxChelator software.

Immunoprecipitation and Western blot
Cell lysates (2–5 mg/ml) or isolated LEL fractions (lysed with 0.1–0.5% Triton X-100) were incubated with 80 µl of 50% protein A/G–agarose beads in PBS for 15 min at 4°C to reduce background proteins that nonspecifically bound to the beads. After centrifugation at 12,000 g for 15 min to remove the beads, aliquots of cell lysates (1–2 mg protein) were incubated with the desired antibodies (3–4 µg) or control IgG at 4°C overnight in a final volume of 1 ml radioimmunoprecipitation assay–PBS buffer with constant rocking. After antibody incubation, protein A/G–agarose beads were added, and the samples were incubated at 4°C for 4 h followed by centrifugation at 1,500 rpm for 10 min at 4°C. The beads were then washed three times with precooled radioimmunoprecipitation assay without proteinase inhibitors and each time centrifuged at 1,500 rpm for 10 min at 4°C. Immune complexes were resolved by SDS-PAGE and subjected to immunoblotting. Proteins were analyzed by standard Western analysis methods.

LEL isolation by subcellular fractionation
LELs were isolated as described previously (Graves et al., 2008; Dong et al., 2010). In brief, cell lysates were obtained by Dounce homogenization in a homogenizing buffer (HM buffer; 0.25 M sucrose, 1 mM EDTA, and 10 mM Hepes, pH 7.0), and then centrifuged at 1,500 g (4,200 rpm, ST-16R, F15 rotor; Thermo Fisher Scientific) at 4°C for 10 min to remove the nuclei and intact cells. Postnuclear supernatants were then subjected to ultracentrifugation through a Percoll density gradient using an ultracentrifuge (Optima L-90K; Beckman Coulter). An ultracentrifuge tube was layered with 2.5 M sucrose, 18% Percoll in HM buffer, and supernatant (top). The centrifugation was performed at 90,000 g (31,300 rpm), 4°C, for 1 h using a rotor (70.1 Ti; Beckman Coulter). Samples were fractionated into light, medium, and heavy membrane fractions. Heavy membrane fractions contained concentrated bands of cellular organelles and were further layered over a discontinuous iodixanol gradient, generated by mixing iodixanol in HM buffer with 2.5 M glucose (in vol/vol; 27%, 22.5%, 19%, 16%, 12%, and 8%) and with osmolarity maintained at 300 mOsm for all solutions. After centrifugation at 4°C for 2.5 h at 180,000 g (44,200 rpm), each sample was divided into twelve fractions (0.5 ml each) for further analyses. Note, the biological and ionic compositions of the LELs were largely maintained as a result of the low rate of transport across the LEL membrane at 4°C.

Lysosomal electrophysiology
Lysosomal electrophysiology was performed in isolated enlarged LELs using a modified patch–clamp method as described previously (Dong et al., 2008, 2009). In brief, cells were treated with 1 µM vacuolin-1, a lipophilic polycyclic triazine that can selectively increase the size of LELs (Huynh and Andrews, 2005), for >2 h. Large vacuoles were observed in most vacuolin-1–treated cells. Enlarged vacuoles were also seen in nontreated P2X4-expressing cells, and no obvious difference in P2X4 channel properties was detected between enlarged vacuoles obtained with or without vacuolin-1 treatment. Whole-lysosome recordings were performed on manually isolated enlarged LELs (Dong et al., 2010). In brief, a patch pipette was pressed against a cell and quickly pulled away to slice the cell membrane. This allowed enlarged LELs to be released into the recording chamber and identified by monitoring EGFP fluorescence. After formation of a gigaseal between the patch pipette and an enlarged LEL, capacitance transients were compensated. Voltage steps of several hundred millivolts with millisecond durations were then applied to break the patched membrane and establish the whole-lysosome configuration.

Unless otherwise stated, bath (cytoplasmic) solution contained 140 mM K-gluconate, 4 mM NaCl, 1 mM EGTA, 2 mM MgCl$_2$, 0.39 mM CaCl$_2$, and 20 mM Hepes (pH was adjusted with KOH to 7.2; free [Ca^{2+}] was 100 nM). The pipette (luminal) solution was a standard extracellular solution (modified Tyrode's: 145 mM NaCl, 5 mM KCl, 2 mM CaCl$_2$, 1 mM MgCl$_2$, 10 mM Hepes, and 10 mM glucose; the pH was adjusted with HCl and NaOH to 4.6 or 7.4). Data were collected using a patch–clamp amplifier (Axopatch 2A), Digidata 1440, and pClamp 10.2 software (Axon Instruments). Whole-lysosome currents were digitized at 10 kHz and filtered at 2 kHz. All experiments were conducted at room temperature (21–23°C), and all recordings were analyzed with pClamp 10.2 and Origin 8.0 (OriginLab).

Vacuole assay
Cos1 cells were transiently transfected with P2X4 and/or its mutants or other desired cDNAs. Nontransfected cells or cells transfected with Lamp1 were used as controls. At 24 h after transfection, cells on coverslips were loaded with Texas red 10-kD dextran (1 mg/ml) in complete medium for 3 h and chased for 2 h. Cells then were treated with various chemicals as indicated. After the treatment, they were fixed immediately, and coverslips were mounted to glass slides. All images were taken using a confocal microscope (Meta510; Carl Zeiss). Normally, the majority of LEL have sizes with diameters <0.5 µm, which are hard to resolve with light microscopy. For quantification, cells were counted as vacuolated if there were more than three enlarged (>2 µm in diameter for Cos1 and >1 µm in diameter for C2C12) cytoplasmic vacuoles, with the vacuole sizes determined using ZEN 2012 program (Carl Zeiss). Percentage of vacuolated cells in each experiment was calculated from counting ≥250 cells from randomly chosen fields, and the experiments were repeated three times (n = 3). Live-cell images were obtained at room temperature using the EasyRatioPro system.

TEM
Cell pellets of Cos1 cells were used for these experiments. First, cells were fixed in 2.5% glutaraldehyde in 0.1 M sodium cacodylate buffer, pH 7.4, for 2–12 h. After fixation, cells were gently scraped and centrifuged into cell pellets. Cell pellets were then immersed in 1% osmium tetroxide in buffered saline. Pellets were then rinsed quickly with distilled water and followed by staining with 0.25% uranyl acetate at 4°C overnight. Further dehydration was performed in a series of acetone dehydration steps (50% for 10 min, 70% for 10 min ×2, 95% for 10 min ×2, and 100% for 10 min ×2) and dried with 100% acetone for 10 min. Infiltration was performed by a 3:1 mixture of dried 100% acetone and resin for 3 h and then a 1:3 mixture of dried 100% acetone and resin overnight. Embedding was performed in 100% Epon Araldite Resin for 3 h ×2 and followed by drying in an oven at 60°C for 48 h. Thin sections (100 nm) were then cut using an ultramicrotome (Huxley; LKB Instruments, Inc.) with a diamond knife and placed on 300 mesh copper grids. Grids were stained with lead citrate. Samples were viewed with a transmission electron microscope (JEM 1230; JEOL) at 80 kV. Images were captured using a digital camera (ORCA-HR; Hamamatsu Photonics). Lysosome sizes were measured using the Advanced Microscopy Techniques image capture engine.

Knockout of P2X4 and ALG-2 using CRISPR-Cas9 system
The operation followed detailed instructions of the published protocol (Cong et al., 2013). In brief, 20-bp target single-guide RNA sequences were obtained by screening P2X4 mRNA sequence with CRISPR DESIGN online software (http://crispr.mit.edu/), and two sequences were chosen: 5′-AGTCCCGAGTGTCGAGGCGC-3′ (target 1) and 5′-GGGTGCTGTTATGGACGTGT-3′ (target 2). After being annealed with their reverse complementary sequences, the short double-strand

DNAs were ligated with Bbs I–digested pX330-2A-GFP that was generously provided by L. Mei, and the new constructs were named pX330-2A-GFP/P2X4-1 and -2, respectively. For ALG-2, the chosen guide RNA sequences were 5′-GCTGCCTACTCCTACCGCCC-3′ (target 1) and 5′-TGTCTTCCGGACCTACGACA-3′ (target 2), the annealed DNAs were further ligated with Bbs I–digested pX330-2A-GFP, and the new constructs were named pX330-2A-GFP/ALG2-1 and -2, respectively. C2C12 cells were transfected with individual pX330-2A-GFP/P2X4 using the Neon system (Life Technologies) following optimized protocol and cultured for 72 h before use. The transfection efficiency for C2C12 cells was >90%.

Cell-free fusion assay
Cos1 cells were transiently transfected with Lamp1-mCherry, Lamp1-GFP, P2X4-mCherry (or P2X4-DsRed), or P2X4-GFP. Efficiency of each transfection was controlled to be comparable (∼75%) among groups. At 24 h after transfection, 1.5×10^7 cells of each group were used for further collection of PNF. In brief, cells were suspended in 1.5 ml cytoplasmic solution containing 140 mM K-gluconate, 4 mM NaCl, 1 mM EGTA, 2 mM MgCl$_2$, 0.39 mM CaCl$_2$, and 20 mM Hepes (pH was adjusted with KOH to 7.2; free [Ca^{2+}] was 100 nM). Cells were homogenized with a Dounce homogenizer to reach ∼75% cell breakage to avoid excessive organelle damage. Homogenized cells were centrifuged at 1,500 g (4,200 rpm; ST-16R, F15 rotor) at 4°C for 10 min to remove the nuclei and intact cells. PNFs were collected and used for further cell-free fusion assay.

The volume of PNF from each group was finalized to 1.5 ml with the cytoplasmic solution. Lamp1 and P2X4 were, if not exclusively, predominantly expressed on LEL; therefore, fluorescent vesicles would represent LEL. 50 µl PNF containing GFP or mCherry (or DsRed) vesicles were placed in a 0.05% poly-lysine–coated glass bottom chamber and allowed to sediment for 30 min on ice. Vesicles in PNF were viewed, and particle numbers were counted using ImageJ particle analysis. Density of GFP or mCherry (or DsRed) vesicles were adjusted to ∼550 per field (∼50 per image showed) before mixture. After adjusting, GFP and mCherry (or DsRed) PNF were mixed thoroughly at a ratio of 1:1 by pipetting gently for 10 times. All cell-free assays were performed under this density, which was designated as high density (original density) in the density fusion experiment. For the medium density group, the mixture was diluted with the cytoplasmic solution at a ratio of 1:5; for the low density group, the mixture was diluted with the cytoplasmic solution at a ratio of 1:25.

For cell-free assay treatment, PNF mixture was incubated at 37°C in a 0.05% poly-lysine–coated glass bottom chamber. 2 mM ATP was added in the mixture to provide energy source for fusion. The mixture was incubated at 37°C for 1 h with or without 10 mM MA. In some experiments, 10 µM BAPTA, 3 µM W7, or 20 µM Cu^{2+} was simultaneously added with MA as inhibitors. For each sample, ≥10 areas were randomly chosen for imaging. Fused vesicles were identified as yellow puncta, i.e., the colocalization of GFP with mCherry/DsRed fluorescence, in merged images. Colocalization was analyzed using ImageJ. Analysis was performed by a person blinded to the experiment. Experiments were repeated three times with triplicated samples each time.

Data analysis
Data are presented as means ± SEM. Statistical comparisons were made using analysis of variance and Student's t test. P-values of <0.05 were considered statistically significant. *, P < 0.05; **, P < 0.01.

Online supplemental material
Fig. S1 shows time-dependent vacuole enlargement induced by P2X4 activation. Fig. S2 shows that patch-clamp recording of P2X4 and its

mutants. Fig. S3 shows that LEL biogenesis was not affected with inducing or blocking vacuolation. Fig. S4 shows that Syt VII and ALG-2 was not involved in vacuolation induced by P2X4 activation. Fig. S5 shows concentration- and time-dependent LEL fusion in cell-free system. Online supplemental material is available at http://www.jcb.org/cgi/content/full/jcb.201409071/DC1.

References

Baars, T.L., S. Petri, C. Peters, and A. Mayer. 2007. Role of the V-ATPase in regulation of the vacuolar fission-fusion equilibrium. *Mol. Biol. Cell.* 18:3873–3882. http://dx.doi.org/10.1091/mbc.E07-03-0205

Bakker, A.C., P. Webster, W.A. Jacob, and N.W. Andrews. 1997. Homotypic fusion between aggregated lysosomes triggered by elevated [Ca2+]i in fibroblasts. *J. Cell Sci.* 110:2227–2238.

Brandhorst, D., D. Zwilling, S.O. Rizzoli, U. Lippert, T. Lang, and R. Jahn. 2006. Homotypic fusion of early endosomes: SNAREs do not determine fusion specificity. *Proc. Natl. Acad. Sci. USA.* 103:2701–2706. http://dx.doi.org/10.1073/pnas.0511138103

Calcraft, P.J., M. Ruas, Z. Pan, X. Cheng, A. Arredouani, X. Hao, J. Tang, K. Rietdorf, L. Teboul, K.T. Chuang, et al. 2009. NAADP mobilizes calcium from acidic organelles through two-pore channels. *Nature.* 459:596–600. http://dx.doi.org/10.1038/nature08030

Cang, C., Y. Zhou, B. Navarro, Y.J. Seo, K. Aranda, L. Shi, S. Battaglia-Hsu, I. Nissim, D.E. Clapham, and D. Ren. 2013. mTOR regulates lysosomal ATP-sensitive two-pore Na(+) channels to adapt to metabolic state. *Cell.* 152:778–790. http://dx.doi.org/10.1016/j.cell.2013.01.023

Cao, Q., K. Zhao, X.Z. Zhong, Y. Zou, H. Yu, P. Huang, T.L. Xu, and X.P. Dong. 2014. SLC17A9 protein functions as a lysosomal ATP transporter and regulates cell viability. *J. Biol. Chem.* 289:23189–23199. http://dx.doi.org/10.1074/jbc.M114.567107

Chen, C.S., G. Bach, and R.E. Pagano. 1998. Abnormal transport along the lysosomal pathway in mucolipidosis, type IV disease. *Proc. Natl. Acad. Sci. USA.* 95:6373–6378. http://dx.doi.org/10.1073/pnas.95.11.6373

Cheng, X., D. Shen, M. Samie, and H. Xu. 2010. Mucolipins: Intracellular TRPML1-3 channels. *FEBS Lett.* 584:2013–2021. http://dx.doi.org/10.1016/j.febslet.2009.12.056

Christensen, K.A., J.T. Myers, and J.A. Swanson. 2002. pH-dependent regulation of lysosomal calcium in macrophages. *J. Cell Sci.* 115:599–607.

Clarke, C.E., C.D. Benham, A. Bridges, A.R. George, and H.J. Meadows. 2000. Mutation of histidine 286 of the human P2X4 purinoceptor removes extracellular pH sensitivity. *J. Physiol.* 523:697–703. http://dx.doi.org/10.1111/j.1469-7793.2000.00697.x

Coddou, C., B. Morales, J. González, M. Grauso, F. Gordillo, P. Bull, F. Rassendren, and J.P. Huidobro-Toro. 2003. Histidine 140 plays a key role in the inhibitory modulation of the P2X4 nucleotide receptor by copper but not zinc. *J. Biol. Chem.* 278:36777–36785. http://dx.doi.org/10.1074/jbc.M305177200

Colombo, M.I., W. Beron, and P.D. Stahl. 1997. Calmodulin regulates endosome fusion. *J. Biol. Chem.* 272:7707–7712. http://dx.doi.org/10.1074/jbc.272.12.7707

Cong, L., F.A. Ran, D. Cox, S. Lin, R. Barretto, N. Habib, P.D. Hsu, X. Wu, W. Jiang, L.A. Marraffini, and F. Zhang. 2013. Multiplex genome engineering using CRISPR/Cas systems. *Science.* 339:819–823. http://dx.doi.org/10.1126/science.1231143

Dong, X.P., X. Cheng, E. Mills, M. Delling, F. Wang, T. Kurz, and H. Xu. 2008. The type IV mucolipidosis-associated protein TRPML1 is an endolysosomal iron release channel. *Nature.* 455:992–996. http://dx.doi.org/10.1038/nature07311

Dong, X.P., X. Wang, D. Shen, S. Chen, M. Liu, Y. Wang, E. Mills, X. Cheng, M. Delling, and H. Xu. 2009. Activating mutations of the TRPML1 channel revealed by proline-scanning mutagenesis. *J. Biol. Chem.* 284:32040–32052. http://dx.doi.org/10.1074/jbc.M109.037184

Dong, X.P., D. Shen, X. Wang, T. Dawson, X. Li, Q. Zhang, X. Cheng, Y. Zhang, L.S. Weisman, M. Delling, and H. Xu. 2010. PI(3,5)P(2) controls membrane trafficking by direct activation of mucolipin Ca(2+) release channels in the endolysosome. *Nat. Commun.* 1:38. http://dx.doi.org/10.1038/ncomms1037

Efe, J.A., R.J. Botelho, and S.D. Emr. 2005. The Fab1 phosphatidylinositol kinase pathway in the regulation of vacuole morphology. *Curr. Opin. Cell Biol.* 17:402–408. http://dx.doi.org/10.1016/j.ceb.2005.06.002

Graves, A.R., P.K. Curran, C.L. Smith, and J.A. Mindell. 2008. The Cl-/H+ antiporter ClC-7 is the primary chloride permeation pathway in lysosomes. *Nature.* 453:788–792. http://dx.doi.org/10.1038/nature06907

Grimm, C., L.M. Holdt, C.C. Chen, S. Hassan, C. Müller, S. Jörs, H. Cuny, S. Kissing, B. Schröder, E. Butz, et al. 2014. High susceptibility to fatty liver disease in two-pore channel 2-deficient mice. *Nat. Commun.* 5:4699. http://dx.doi.org/10.1038/ncomms5699

Guo, C., M. Masin, O.S. Qureshi, and R.D. Murrell-Lagnado. 2007. Evidence for functional P2X4/P2X7 heteromeric receptors. *Mol. Pharmacol.* 72:1447–1456. http://dx.doi.org/10.1124/mol.107.035980

Hay, J.C. 2007. Calcium: a fundamental regulator of intracellular membrane fusion? *EMBO Rep.* 8:236–240. http://dx.doi.org/10.1038/sj.embor.7400921

Huang, P., Y. Zou, X.Z. Zhong, Q. Cao, K. Zhao, M.X. Zhu, R. Murrell-Lagnado, and X.P. Dong. 2014. P2X4 forms functional ATP-activated cation channels on lysosomal membranes regulated by luminal pH. *J. Biol. Chem.* 289:17658–17667. http://dx.doi.org/10.1074/jbc.M114.552158

Huynh, C., and N.W. Andrews. 2005. The small chemical vacuolin-1 alters the morphology of lysosomes without inhibiting Ca2+-regulated exocytosis. *EMBO Rep.* 6:843–847. http://dx.doi.org/10.1038/sj.embor.7400495

Khakh, B.S., and R.A. North. 2012. Neuromodulation by extracellular ATP and P2X receptors in the CNS. *Neuron.* 76:51–69. http://dx.doi.org/10.1016/j.neuron.2012.09.024

Lange, I., S. Yamamoto, S. Partida-Sanchez, Y. Mori, A. Fleig, and R. Penner. 2009. TRPM2 functions as a lysosomal Ca2+-release channel in β cells. *Sci. Signal.* 2:ra23. http://dx.doi.org/10.1126/scisignal.2000278

Lin-Moshier, Y., M.V. Keebler, R. Hooper, M.J. Boulware, X. Liu, D. Churamani, M.E. Abood, T.F. Walseth, E. Brailoiu, S. Patel, and J.S. Marchant. 2014. The Two-pore channel (TPC) interactome unmasks isoform-specific roles for TPCs in endolysosomal morphology and cell pigmentation. *Proc. Natl. Acad. Sci. USA.* 111:13087–13092. http://dx.doi.org/10.1073/pnas.1407004111

Lloyd-Evans, E., and F.M. Platt. 2011. Lysosomal Ca(2+) homeostasis: role in pathogenesis of lysosomal storage diseases. *Cell Calcium.* 50:200–205. http://dx.doi.org/10.1016/j.ceca.2011.03.010

Luzio, J.P., N.A. Bright, and P.R. Pryor. 2007a. The role of calcium and other ions in sorting and delivery in the late endocytic pathway. *Biochem. Soc. Trans.* 35:1088–1091. http://dx.doi.org/10.1042/BST0351088

Luzio, J.P., P.R. Pryor, and N.A. Bright. 2007b. Lysosomes: fusion and function. *Nat. Rev. Mol. Cell Biol.* 8:622–632. http://dx.doi.org/10.1038/nrm2217

Martinez, I., S. Chakrabarti, T. Hellevik, J. Morehead, K. Fowler, and N.W. Andrews. 2000. Synaptotagmin VII regulates Ca2+-dependent exocytosis

of lysosomes in fibroblasts. *J. Cell Biol.* 148:1141–1150. http://dx.doi.org/10.1083/jcb.148.6.1141

Miklavc, P., N. Mair, O.H. Wittekindt, T. Haller, P. Dietl, E. Felder, M. Timmler, and M. Frick. 2011. Fusion-activated Ca2+ entry via vesicular P2X4 receptors promotes fusion pore opening and exocytotic content release in pneumocytes. *Proc. Natl. Acad. Sci. USA.* 108:14503–14508. http://dx.doi.org/10.1073/pnas.1101039108

Moreau, K., B. Ravikumar, M. Renna, C. Puri, and D.C. Rubinsztein. 2011. Autophagosome precursor maturation requires homotypic fusion. *Cell.* 146:303–317. http://dx.doi.org/10.1016/j.cell.2011.06.023

Morgan, A.J., F.M. Platt, E. Lloyd-Evans, and A. Galione. 2011. Molecular mechanisms of endolysosomal Ca2+ signalling in health and disease. *Biochem. J.* 439:349–374. http://dx.doi.org/10.1042/BJ20110949

Nielsen, T.B., J.B. Field, and J.R. Dedman. 1987. Association of calmodulin with lysosomes. *J. Cell Sci.* 87:327–336.

Ogunbayo, O.A., Y. Zhu, B. Shen, E. Agbani, J. Li, J. Ma, M.X. Zhu, and A.M. Evans. 2015. Organelle-specific subunit interactions of the vertebrate two-pore channel family. *J. Biol. Chem.* 290:1086–1095. http://dx.doi.org/10.1074/jbc.M114.610493

Parkinson, K., A.E. Baines, T. Keller, N. Gruenheit, L. Bragg, R.A. North, and C.R. Thompson. 2014. Calcium-dependent regulation of Rab activation and vesicle fusion by an intracellular P2X ion channel. *Nat. Cell Biol.* 16:87–98. http://dx.doi.org/10.1038/ncb2887

Peri, F., and C. Nüsslein-Volhard. 2008. Live imaging of neuronal degradation by microglia reveals a role for v0-ATPase a1 in phagosomal fusion in vivo. *Cell.* 133:916–927. http://dx.doi.org/10.1016/j.cell.2008.04.037

Peters, C., and A. Mayer. 1998. Ca2+/calmodulin signals the completion of docking and triggers a late step of vacuole fusion. *Nature.* 396:575–580. http://dx.doi.org/10.1038/25133

Piper, R.C., and J.P. Luzio. 2004. CUPpling calcium to lysosomal biogenesis. *Trends Cell Biol.* 14:471–473. http://dx.doi.org/10.1016/j.tcb.2004.07.010

Pittman, J.K. 2011. Vacuolar Ca(2+) uptake. *Cell Calcium.* 50:139–146. http://dx.doi.org/10.1016/j.ceca.2011.01.004

Poole, B., and S. Ohkuma. 1981. Effect of weak bases on the intralysosomal pH in mouse peritoneal macrophages. *J. Cell Biol.* 90:665–669. http://dx.doi.org/10.1083/jcb.90.3.665

Pryor, P.R., B.M. Mullock, N.A. Bright, S.R. Gray, and J.P. Luzio. 2000. The role of intraorganellar Ca^{2+} in late endosome–lysosome heterotypic fusion and in the reformation of lysosomes from hybrid organelles. *J. Cell Biol.* 149:1053–1062. http://dx.doi.org/10.1083/jcb.149.5.1053

Quetglas, S., C. Leveque, R. Miquelis, K. Sato, and M. Seagar. 2000. Ca2+-dependent regulation of synaptic SNARE complex assembly via a calmodulin- and phospholipid-binding domain of synaptobrevin. *Proc. Natl. Acad. Sci. USA.* 97:9695–9700. http://dx.doi.org/10.1073/pnas.97.17.9695

Qureshi, O.S., A. Paramasivam, J.C. Yu, and R.D. Murrell-Lagnado. 2007. Regulation of P2X4 receptors by lysosomal targeting, glycan protection and exocytosis. *J. Cell Sci.* 120:3838–3849. http://dx.doi.org/10.1242/jcs.010348

Rong, Y., M. Liu, L. Ma, W. Du, H. Zhang, Y. Tian, Z. Cao, Y. Li, H. Ren, C. Zhang, et al. 2012. Clathrin and phosphatidylinositol-4,5-bisphosphate regulate autophagic lysosome reformation. *Nat. Cell Biol.* 14:924–934. http://dx.doi.org/10.1038/ncb2557

Ruas, M., K. Rietdorf, A. Arredouani, L.C. Davis, E. Lloyd-Evans, H. Koegel, T.M. Funnell, A.J. Morgan, J.A. Ward, K. Watanabe, et al. 2010. Purified TPC isoforms form NAADP receptors with distinct roles for Ca(2+) signaling and endolysosomal trafficking. *Curr. Biol.* 20:703–709. http://dx.doi.org/10.1016/j.cub.2010.02.049

Rudge, S.A., D.M. Anderson, and S.D. Emr. 2004. Vacuole size control: regulation of PtdIns(3,5)P2 levels by the vacuole-associated Vac14-Fig4 complex, a PtdIns(3,5)P2-specific phosphatase. *Mol. Biol. Cell.* 15:24–36. http://dx.doi.org/10.1091/mbc.E03-05-0297

Saftig, P., and J. Klumperman. 2009. Lysosome biogenesis and lysosomal membrane proteins: trafficking meets function. *Nat. Rev. Mol. Cell Biol.* 10:623–635. http://dx.doi.org/10.1038/nrm2745

Samie, M., X. Wang, X. Zhang, A. Goschka, X. Li, X. Cheng, E. Gregg, M. Azar, Y. Zhuo, A.G. Garrity, et al. 2013. A TRP channel in the lysosome regulates large particle phagocytosis via focal exocytosis. *Dev. Cell.* 26:511–524. http://dx.doi.org/10.1016/j.devcel.2013.08.003

Schieder, M., K. Rötzer, A. Brüggemann, M. Biel, and C.A. Wahl-Schott. 2010. Characterization of two-pore channel 2 (TPCN2)-mediated Ca2+ currents in isolated lysosomes. *J. Biol. Chem.* 285:21219–21222. http://dx.doi.org/10.1074/jbc.C110.143123

Shen, D., X. Wang, and H. Xu. 2011. Pairing phosphoinositides with calcium ions in endolysosomal dynamics: phosphoinositides control the direction and specificity of membrane trafficking by regulating the activity of calcium channels in the endolysosomes. *BioEssays.* 33:448–457. http://dx.doi.org/10.1002/bies.201000152

Shen, D., X. Wang, X. Li, X. Zhang, Z. Yao, S. Dibble, X.P. Dong, T. Yu, A.P. Lieberman, H.D. Showalter, and H. Xu. 2012. Lipid storage disorders block lysosomal trafficking by inhibiting a TRP channel and lysosomal calcium release. *Nat. Commun.* 3:731. http://dx.doi.org/10.1038/ncomms1735

Silberberg, S.D., T.H. Chang, and K.J. Swartz. 2005. Secondary structure and gating rearrangements of transmembrane segments in rat P2X4 receptor channels. *J. Gen. Physiol.* 125:347–359. http://dx.doi.org/10.1085/jgp.200409221

Stoop, R., A. Surprenant, and R.A. North. 1997. Different sensitivities to pH of ATP-induced currents at four cloned P2X receptors. *J. Neurophysiol.* 78:1837–1840.

Sumoza-Toledo, A., I. Lange, H. Cortado, H. Bhagat, Y. Mori, A. Fleig, R. Penner, and S. Partida-Sánchez. 2011. Dendritic cell maturation and chemotaxis is regulated by TRPM2-mediated lysosomal Ca2+ release. *FASEB J.* 25:3529–3542. http://dx.doi.org/10.1096/fj.10-178483

Tapper, H., and R. Sundler. 1995. Bafilomycin A1 inhibits lysosomal, phagosomal, and plasma membrane H(+)-ATPase and induces lysosomal enzyme secretion in macrophages. *J. Cell. Physiol.* 163:137–144. http://dx.doi.org/10.1002/jcp.1041630116

Treusch, S., S. Knuth, S.A. Slaugenhaupt, E. Goldin, B.D. Grant, and H. Fares. 2004. *Caenorhabditis elegans* functional orthologue of human protein h-mucolipin-1 is required for lysosome biogenesis. *Proc. Natl. Acad. Sci. USA.* 101:4483–4488. http://dx.doi.org/10.1073/pnas.0400709101

Tsuboi, T., and M. Fukuda. 2007. Synaptotagmin VII modulates the kinetics of dense-core vesicle exocytosis in PC12 cells. *Genes Cells.* 12:511–519. http://dx.doi.org/10.1111/j.1365-2443.2007.01070.x

van den Berghe, P.V., D.E. Folmer, H.E. Malingré, E. van Beurden, A.E. Klomp, B. van de Sluis, M. Merkx, R. Berger, and L.W. Klomp. 2007. Human copper transporter 2 is localized in late endosomes and lysosomes and facilitates cellular copper uptake. *Biochem. J.* 407:49–59. http://dx.doi.org/10.1042/BJ20070705

Vergarajauregui, S., J.A. Martina, and R. Puertollano. 2009. Identification of the penta-EF-hand protein ALG-2 as a Ca2+-dependent interactor of mucolipin-1. *J. Biol. Chem.* 284:36357–36366. http://dx.doi.org/10.1074/jbc.M109.047241

Wang, X., X. Zhang, X.P. Dong, M. Samie, X. Li, X. Cheng, A. Goschka, D. Shen, Y. Zhou, J. Harlow, et al. 2012. TPC proteins are phosphoinositide-activated sodium-selective ion channels in endosomes and lysosomes. *Cell.* 151:372–383. http://dx.doi.org/10.1016/j.cell.2012.08.036

Ward, D.M., J.D. Leslie, and J. Kaplan. 1997. Homotypic lysosome fusion in macrophages: Analysis using an in vitro assay. *J. Cell Biol.* 139:665–673. http://dx.doi.org/10.1083/jcb.139.3.665

Weinert, S., S. Jabs, C. Supanchart, M. Schweizer, N. Gimber, M. Richter, J. Rademann, T. Stauber, U. Kornak, and T.J. Jentsch. 2010. Lysosomal pathology and osteopetrosis upon loss of H+-driven lysosomal Cl-accumulation. *Science.* 328:1401–1403. http://dx.doi.org/10.1126/science.1188072

Xia, X.M., B. Fakler, A. Rivard, G. Wayman, T. Johnson-Pais, J.E. Keen, T. Ishii, B. Hirschberg, C.T. Bond, S. Lutsenko, et al. 1998. Mechanism of calcium gating in small-conductance calcium-activated potassium channels. *Nature.* 395:503–507. http://dx.doi.org/10.1038/26758

Zhao, Y., S. Araki, J. Wu, T. Teramoto, Y.F. Chang, M. Nakano, A.S. Abdelfattah, M. Fujiwara, T. Ishihara, T. Nagai, and R.E. Campbell. 2011. An expanded palette of genetically encoded Ca²+ indicators. *Science.* 333:1888–1891. http://dx.doi.org/10.1126/science.1208592